Materials and Structural Behavior of Basalt Fiber Reinforced Polymer Bars in Bridge Decks

- Mohsen A Issa, Ph.D., PE, SE, FACI, FASCE, FSEI
- Professor of Structural and Materiaks Engineering
- Uiversity of Illinois at Chicago

2025 National Concrete Consortium

Structural Materials Session

Hilton Chicago O'Hare

Rosemont, Illinois

April 9, 2025

Outline

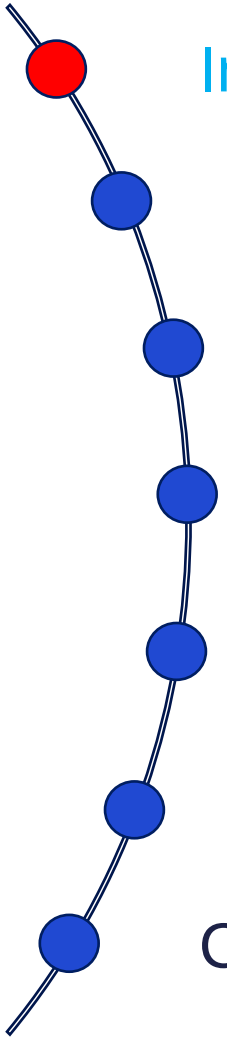

Introduction and Background of Basalt-FRP

Research Approach

Literature Review

Basalt-FRP Material Properties

Structural behavior of Bridge Deck Slabs

Conclusions and Future work

UIC ENGINEERING

Introduction and Objectives

Introduction

- Bridge deck deterioration and FRP materials are of great interest to structural engineers nationally and internationally.
- Most of the research in the literature addresses the mechanical properties of FRP bars or their durability characteristics. **None** of them studied the **effect of the bar size on these characteristics**.
- Bridge deck capacity is controlled by the flexural strength, not the punching shear. This research addresses the bridge deck capacity based on the **flexural analysis**.

Motivation and Objectives

- Understand how BFRP bar sizes influence BFRP bars' durability and mechanical behavior.
- Develop an ultimate strength equation for bridge decks with a span length-to-depth ratio of less than 12.

UIC ENGINEERING

Outline

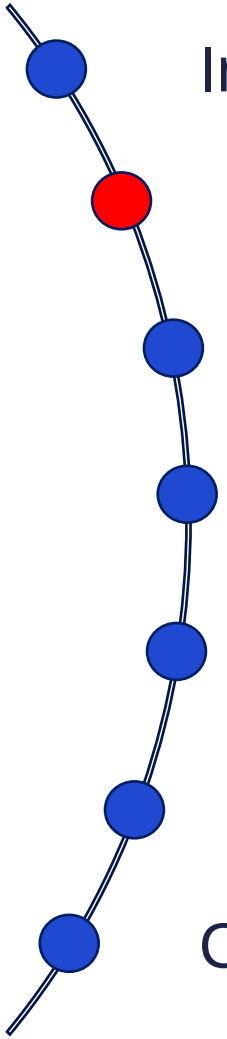

Introduction and Background of Basalt-FRP

Research Objectives

Research Approach

Literature Review

Basalt-FRP Material Properties

Structural behavior of Bridge Deck Slabs

Conclusions and Future work

UIC ENGINEERING

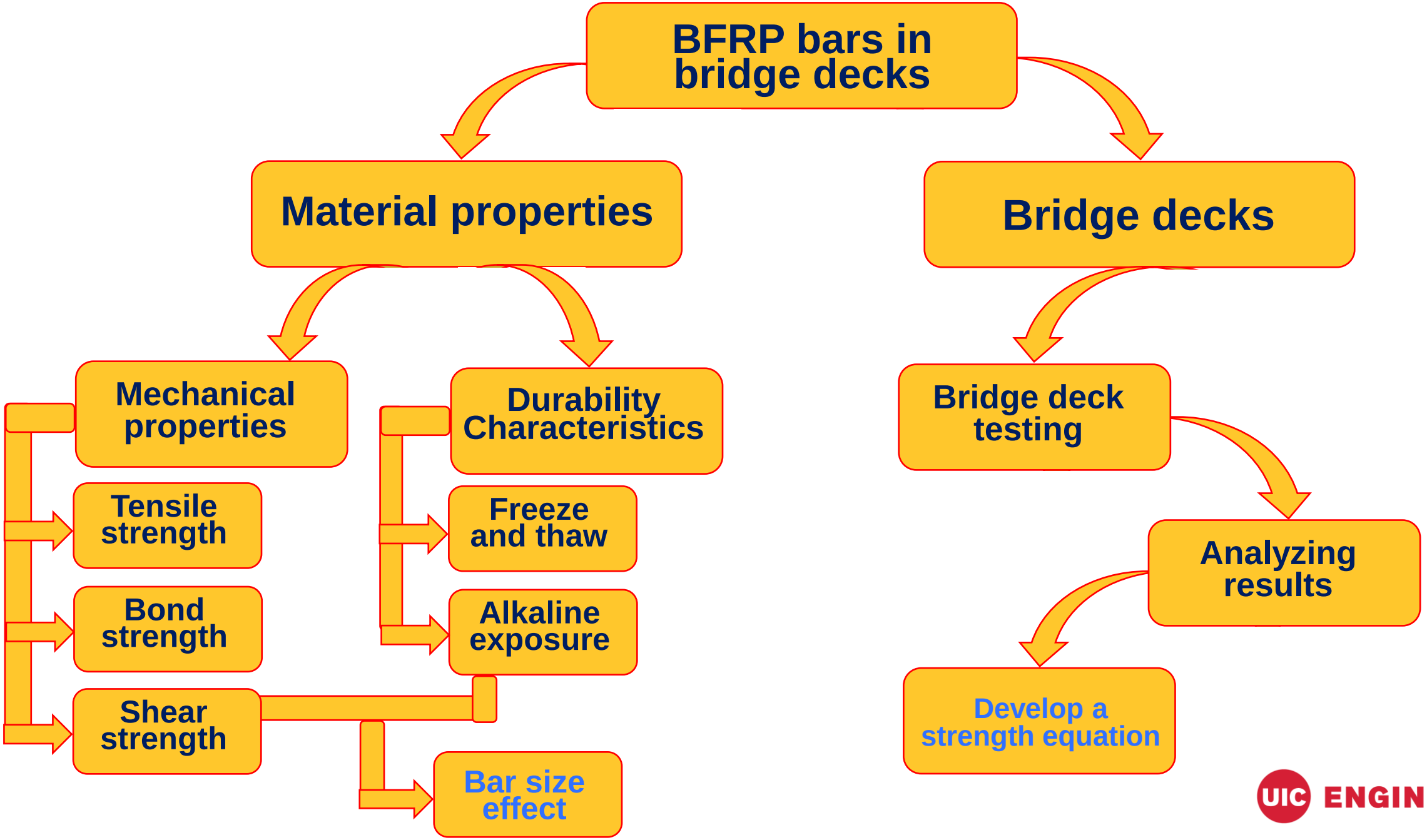

UIC ENGINEERING

WHY FRP bars?

- Tensile strength is greater than steel, an average of 3 times the steel
- In corrosive environment, service life is much greater than steel (ACI440.1R-15)
- Light-weight: one-fourth to one-fifth the weight of steel reinforcing bars
- Less concrete cover if possible
- Admixtures to reduce corrosion are not needed
- High fatigue endurance

UIC ENGINEERING

DISADVANTAGES of FRP bars?

- Lower modulus of elasticity than steel (except Carbon-FRP)
- Weak in the transverse direction
- FRP is linear elastic to failure, whereas steel yields (Elastic-plastic behavior)
- FRP is anisotropic, whereas steel is isotropic
- Endurance time in fire is less than in steel
- No considered compression strength

UIC ENGINEERING

Outline

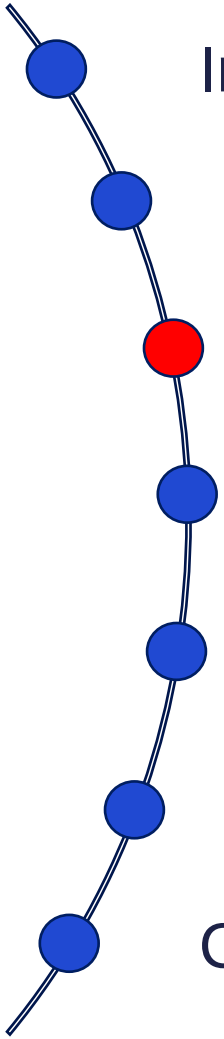

Introduction and Background of Basalt-FRP

Research Objectives

Research Approach

Literature Review

Basalt-FRP Material Properties

Structural behavior of Bridge Deck Slabs

Conclusions and Future work

UIC ENGINEERING

Research Approach

This research aims to study the following:

- Understand the mechanical and durability characteristics:

1. Tensile strength
2. Transverse shear strength
3. Bond strength with concrete
4. Alkali resistance
5. Freeze and thaw resistance

Research Approach

Study the behavior of:

1. Four full-scale single-span bridge decks reinforced with BFRP reinforcing bars
2. Two full-scale, two-span continuous bridge deck slabs reinforced with BFRP bars

Outline

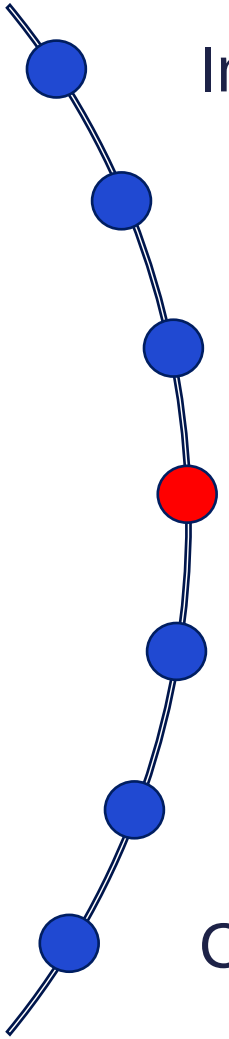

Introduction and Background of Basalt-FRP

Research Objectives

Research Approach

Literature Review

Basalt-FRP Material Properties

Structural behavior of Bridge Deck Slabs

Conclusions and Future work

UIC ENGINEERING

Literature Review

Tensile strength

Many researchers have covered tensile strength and tensile modulus of elasticity of BFRP reinforcement bars and concluded that the stress is not distributed uniformly across the cross-section and is directly proportional to the fiber content.

Bond and shear strength

Bond and shear strength studies examined the bond and shear strength that varies with the variation of the bar surface, fiber source, and the resin material used.

Durability characteristics

Results of the alkaline-resistance experiment show that basalt and glass fibers seem to have typical failure characteristics, drop in strength, and volumetric stability more rapidly than carbon fiber under harsh alkali conditions.

Bridge deck testing

Most of the studies in the literature tested bridge deck slabs for punching shear failure. Other tests study the arch action mechanism of the bridge deck due to the lower length-to-depth ratio. However, concrete bridge deck needs to be studied as a flexural element.

Outline

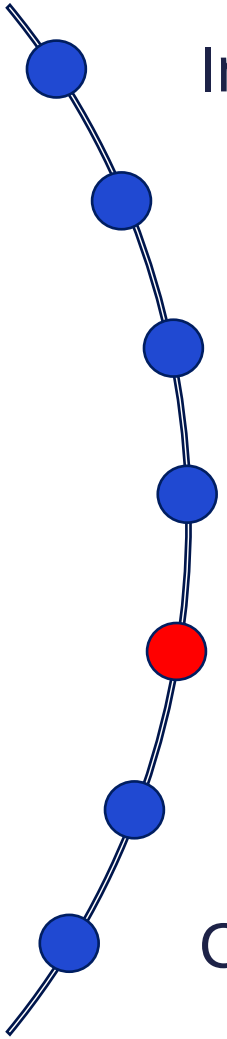

Introduction and Background of Basalt-FRP

Research Objectives

Research Approach

Literature Review

Basalt-FRP Material Properties

Structural behavior of Bridge Deck Slabs

Conclusions and Future work

UIC ENGINEERING

Mechanical and Durability characteristics of Basalt-FRP bars

UIC ENGINEERING

Tensile strength

- Universal tensile testing machine was used for the tensile strength testing, which requires special attention at the end of the bars due to the lower shear strength of Basalt-FRP bars.

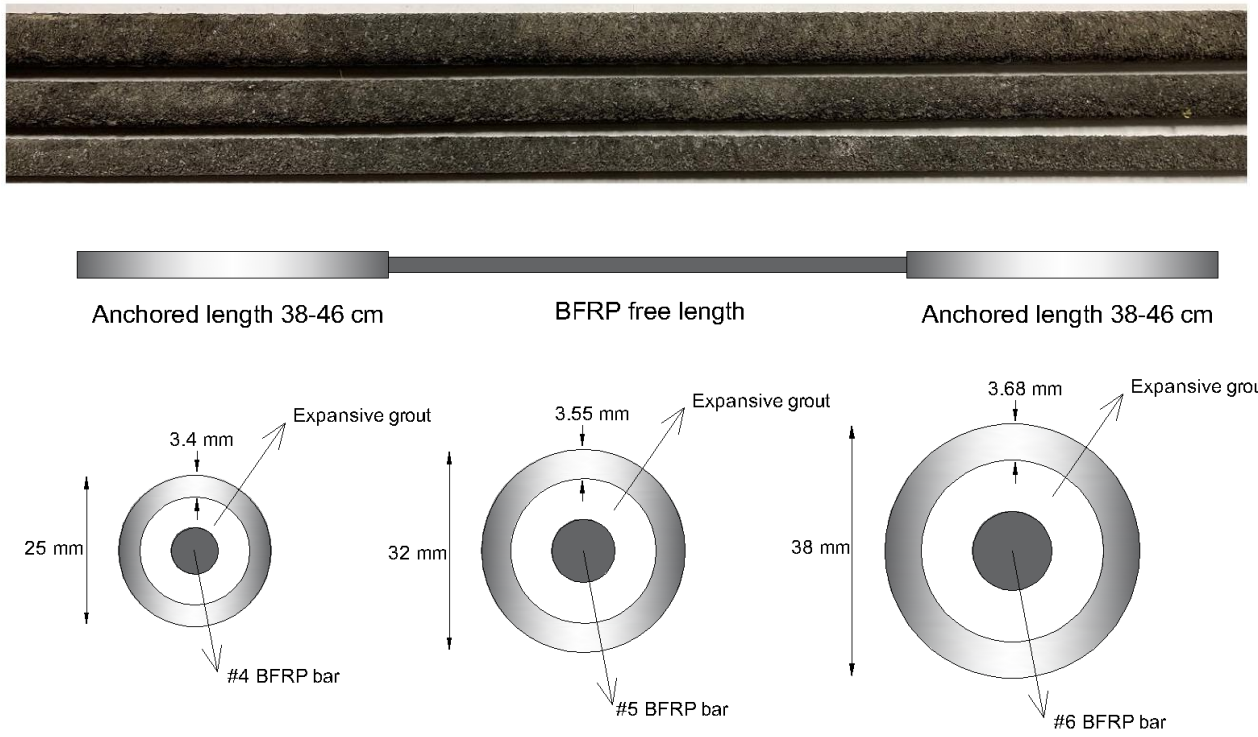

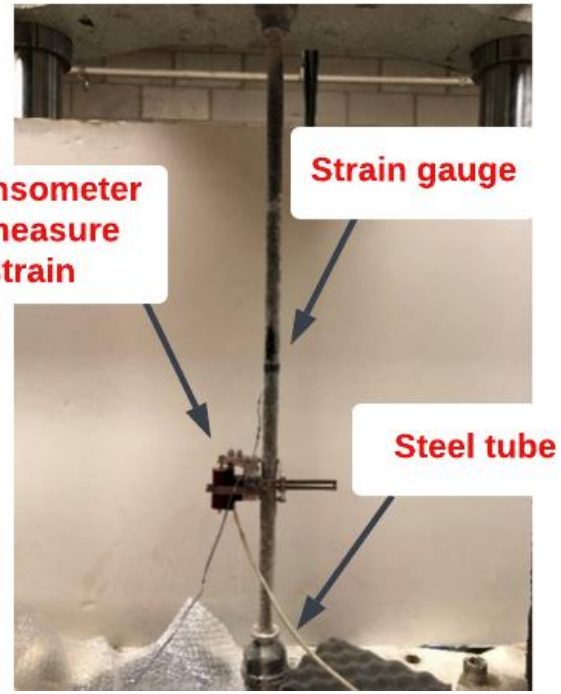

UIC ENGINEERING

Tensile strength

- Testing results showed a linear Stress-Strain relationship of the tested rebars up to failure.

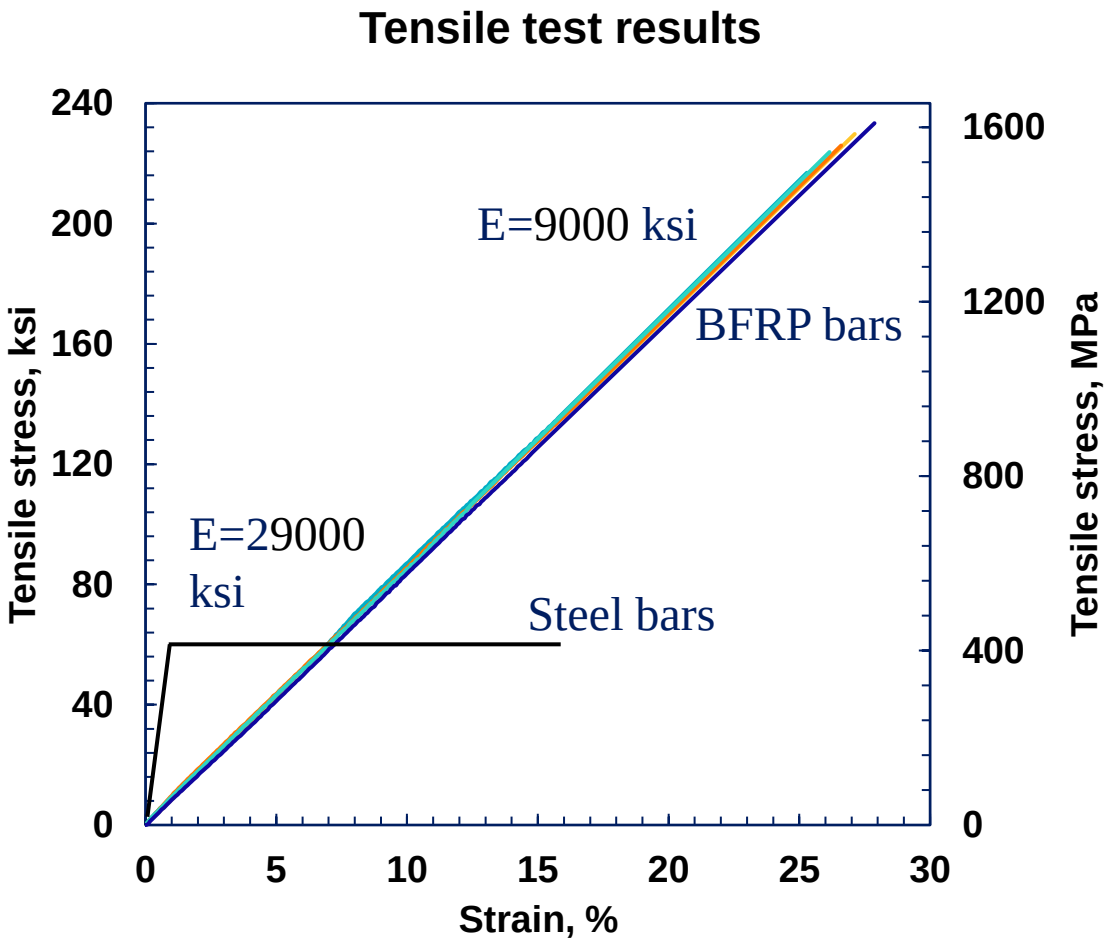

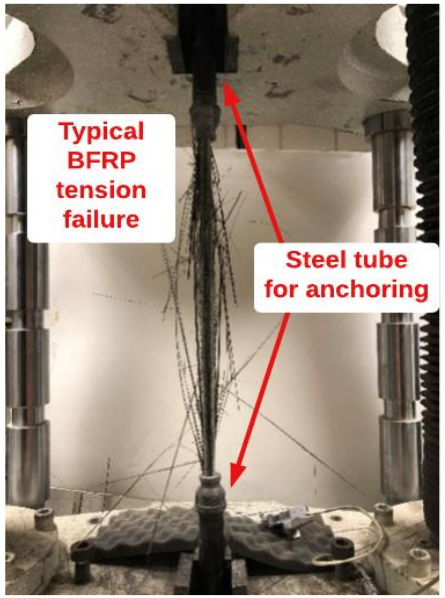

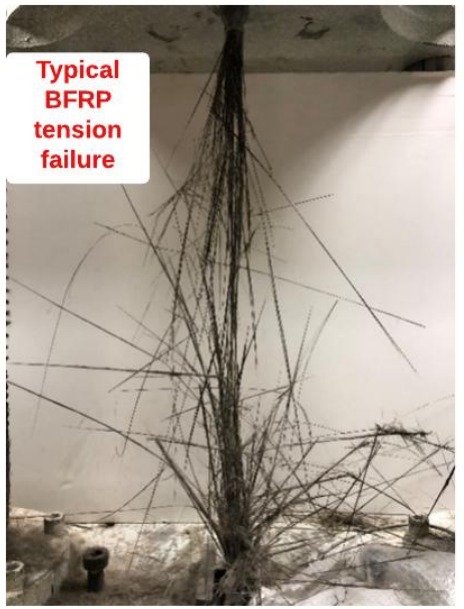

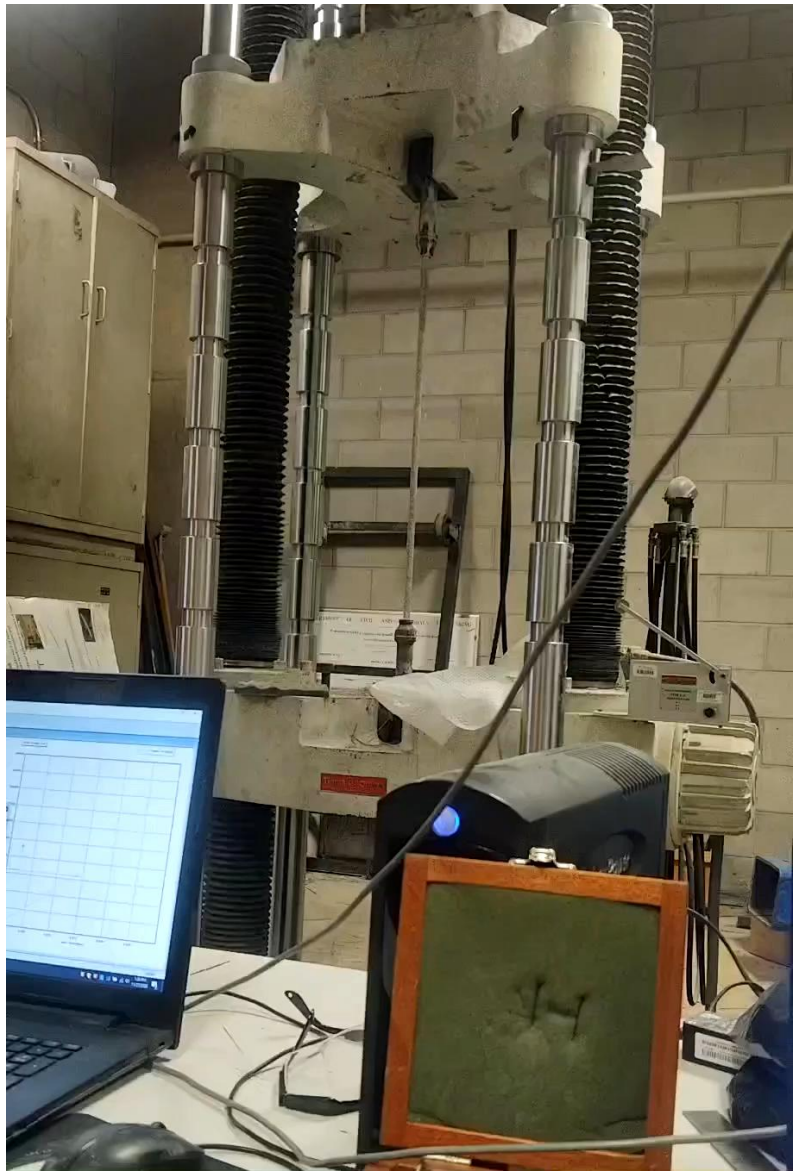

Tensile strength

Bar #	Sample #	Tensile modulus of elasticity, ksi	Average Modulus of Elasticity, ksi	Tensile stress, ksi	Average Tensile stress, ksi	Standard deviation, ksi	Ultimate strain, %	Average Rupture Strain, %
4	Sample 1	8473	**8494**	230	**226**	**5.6**	2.71	**2.66**
	Sample 2	8576		217			2.53	
	Sample 3	8494		226			2.66	
	Sample 4	8372		233			2.78	
	Sample 5	8555		224			2.62	
5	Sample 1	8583	**8674**	209	**202**	**9.5**	2.43	**2.35**
	Sample 2	8695		214			2.45	
	Sample 3	8563		203			2.37	
	Sample 4	8725		197			2.27	
	Sample 5	8802		190			2.26	
6	Sample 1	8713	**8798**	162	**171**	**11.6**	1.87	**1.98**
	Sample 2	8729		175			2.04	
	Sample 3	8808		154			1.78	
	Sample 4	8969		178			2.04	
	Sample 5	8774		186			2.19	

UIC ENGINEERING

Tensile strength

- The tested BFRP rebars showed a very high tensile strength compared to the tested bars in the literature.
- The reason behind this difference is that the bar has no deformation on the surface like steel reinforcement, which means all the fibers are aligned in the vertical direction.

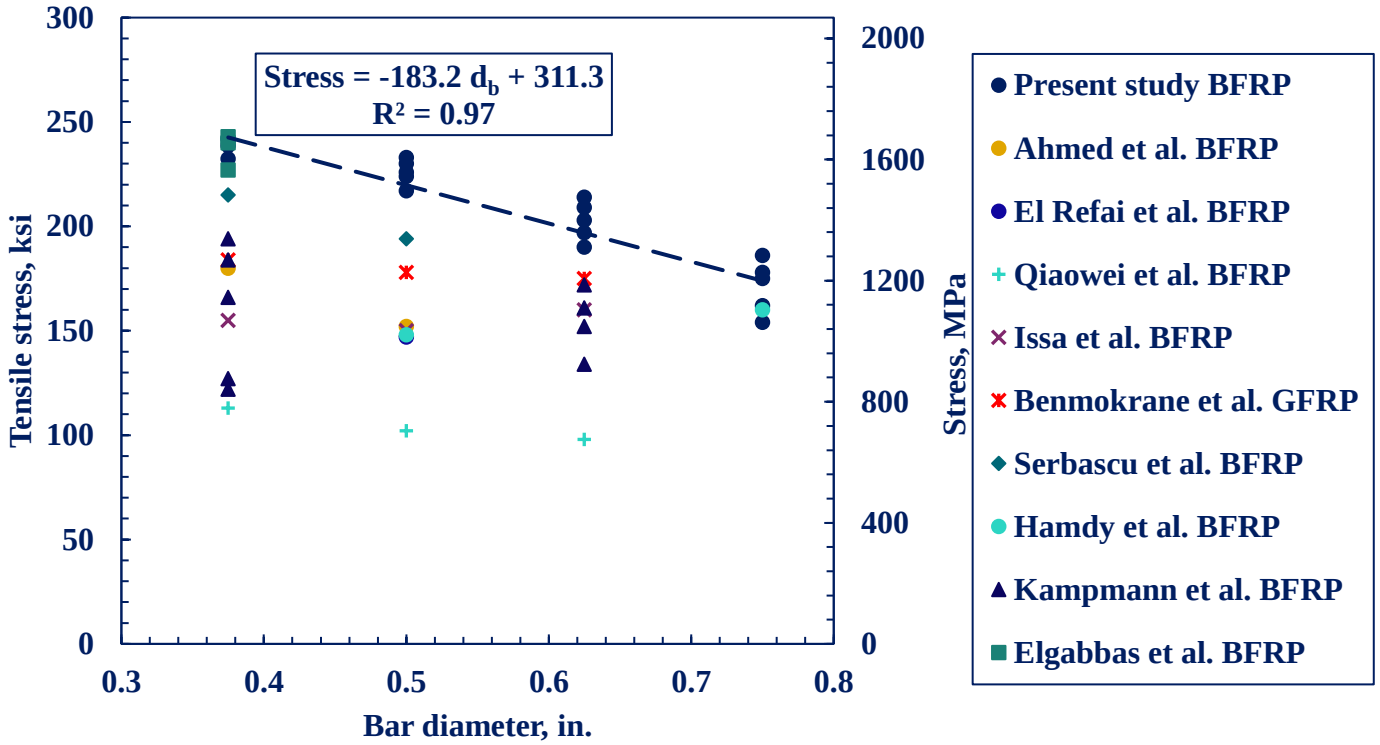

UIC ENGINEERING

Tensile strength (Acceptance criterion)

- Any tensile test results must satisfy the acceptance criterion of tensile strength for better material production and quality control.
- An existing acceptance criterion for tensile strength of GFRP and CFRP bars, without generalization of this criterion for basalt FRP reinforcing bars, is implemented in ACI 440.1R-15.
- The acceptance criterion is the guaranteed tensile strength, the average tensile strength minus three times the standard deviation.

$$f_{fu} = f_{fu,average} - 3\sigma$$

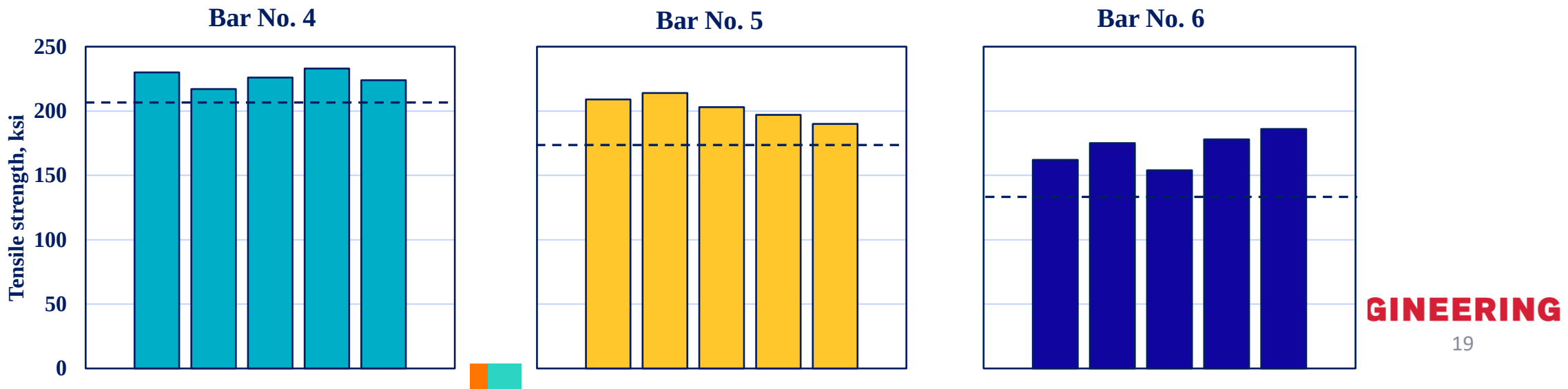

GINEERING

Tensile strength (Acceptance criterion)

- The guaranteed tensile strength corresponds to 99% of confidence (Rossini et al. 2018).
- A 5% reduction in the ultimate strength will ensure 100% confidence.

$$f'_{fu} < 0.95\ f^{*}_{fu}$$

- Kampmann et al. tested five different bar sources and concluded that two bar sources did not match the guaranteed tensile strength requirement by ACI 440.1R.

UIC ENGINEERING

Bond strength

- This test is composed of pulling the bar from an 8” cube of concrete with a bonded length of 5 x bar diameter.

- The bond strength of the BFRP with concrete is calculated according to the following equation:

$$\mu = \frac{P_u}{5\pi {d_b}^2}$$

Where μ: Bond stress, psi,

P_u; Applied load, lb.

d_b BFRP bar diameter, in.

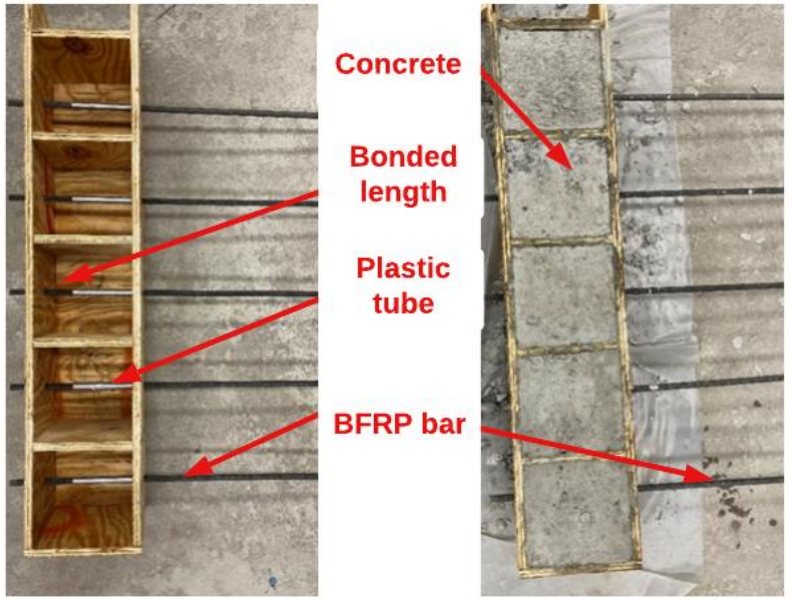

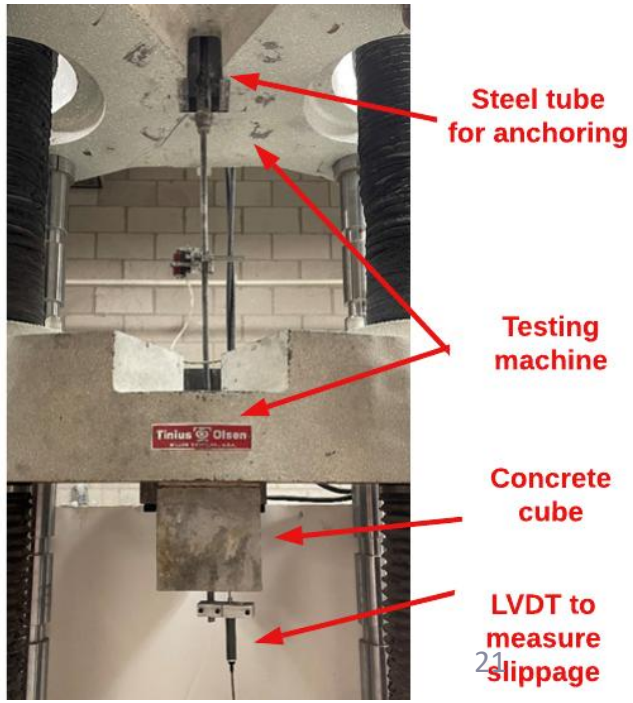

Bond strength

Bar size	Sample No.	Maximum bond stress, psi	Average bond stress, psi	Standard deviation, psi	Coefficient of variation, %
No. 4	1	1402	1484	181.1	12.2
	2	1483			
	3	1524			
	4	1397			
	5	1614			
No. 5	1	1237	1273	101	7.9
	2	1338			
	3	1304			
	4	1212			
	5	1273			
No. 6	1	1215	1147	84.6	7.4
	2	1116			
	3	1163			
	4	1119			
	5	1124			

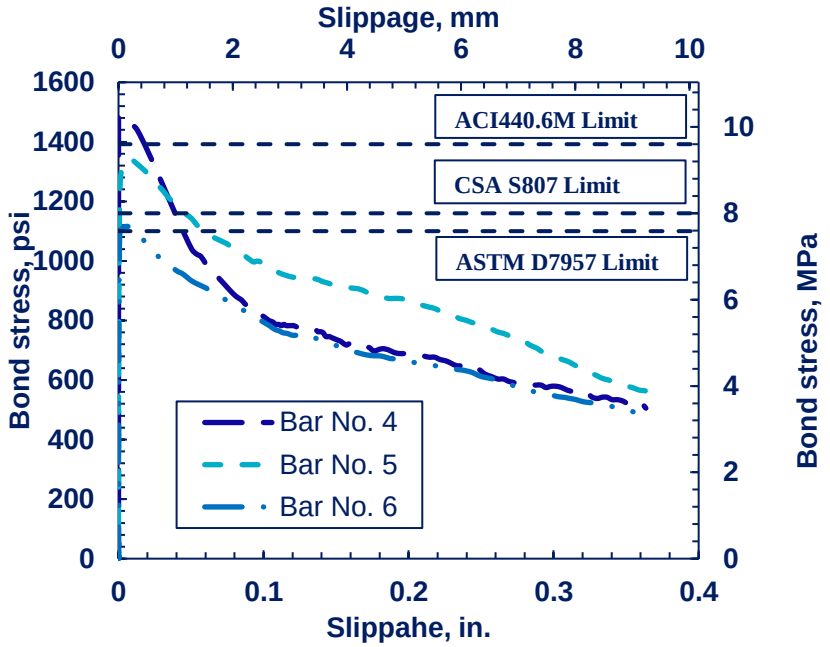

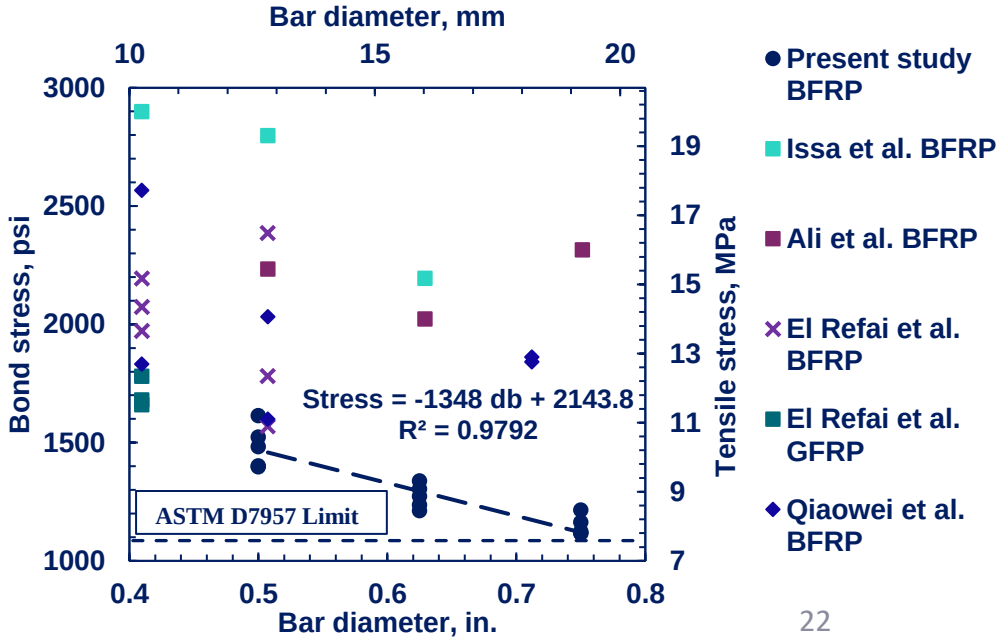

Scientific explanation

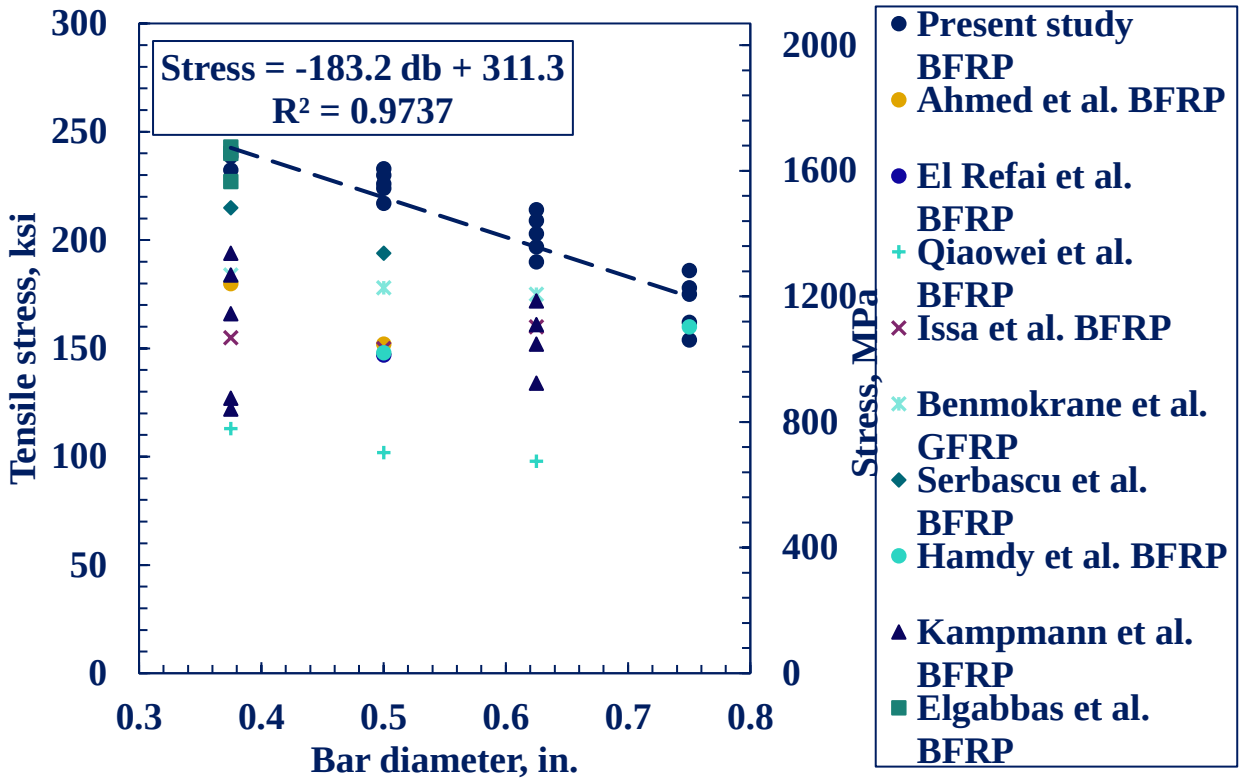

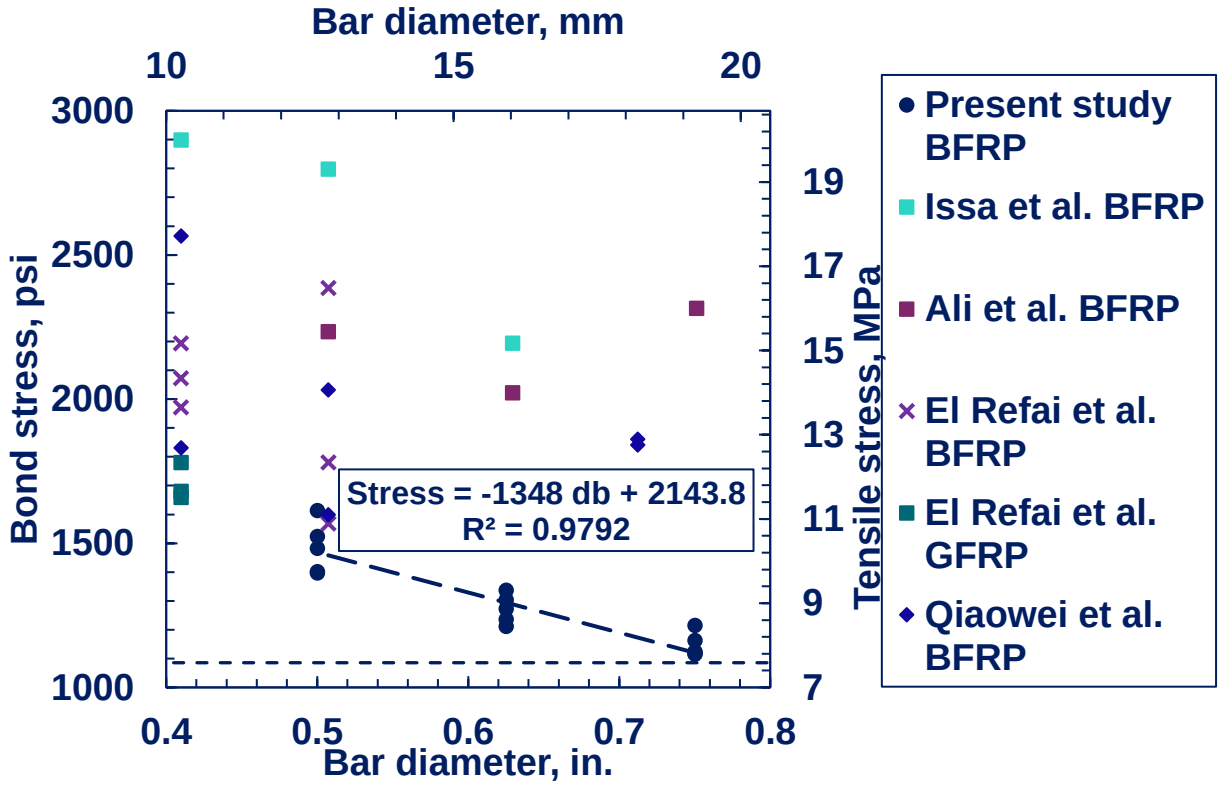

UIC ENGINEERING

Scientific explanation

- BFRP bar is an anisotropic material. Thus, the stress distribution across the section is not uniform.
- This phenomenon is called the shear lag.
- The figure below illustrates the bond stress distribution on the BFRP bar of the deformed and non-deformed surface.

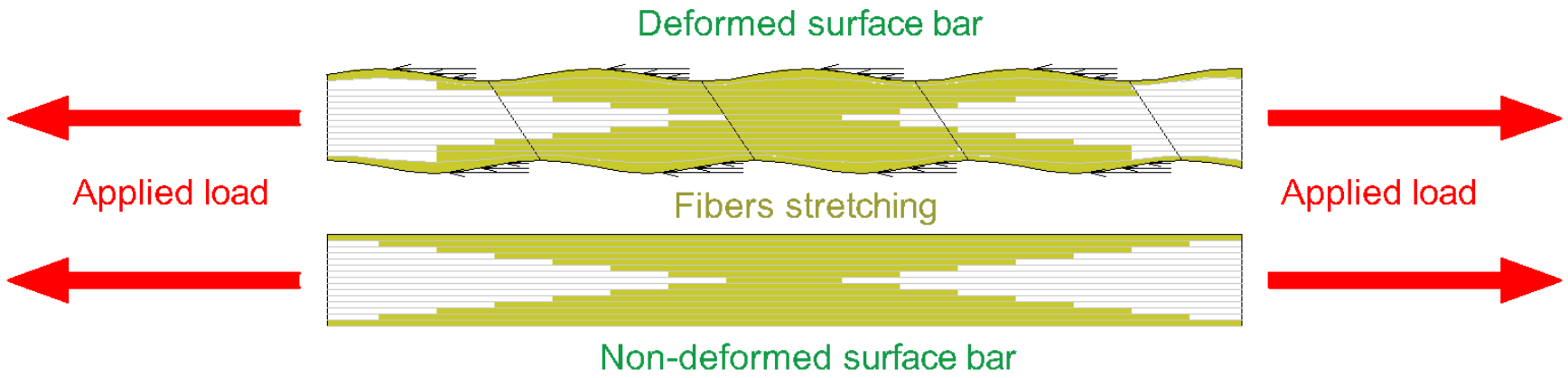

UIC ENGINEERING

Bond strength

- The beams are composed of two separate parts joined with the BFRP bar in the tension zone and a special fixture in the compression zone that allows rotation, as shown in the Figure.

- The tension force in the rebar and the bond stress can be calculated according to the following equations:

- $$T = \frac{Pa}{2L} \quad \text{and} \quad u = \frac{T}{\pi L_a d_b}$$

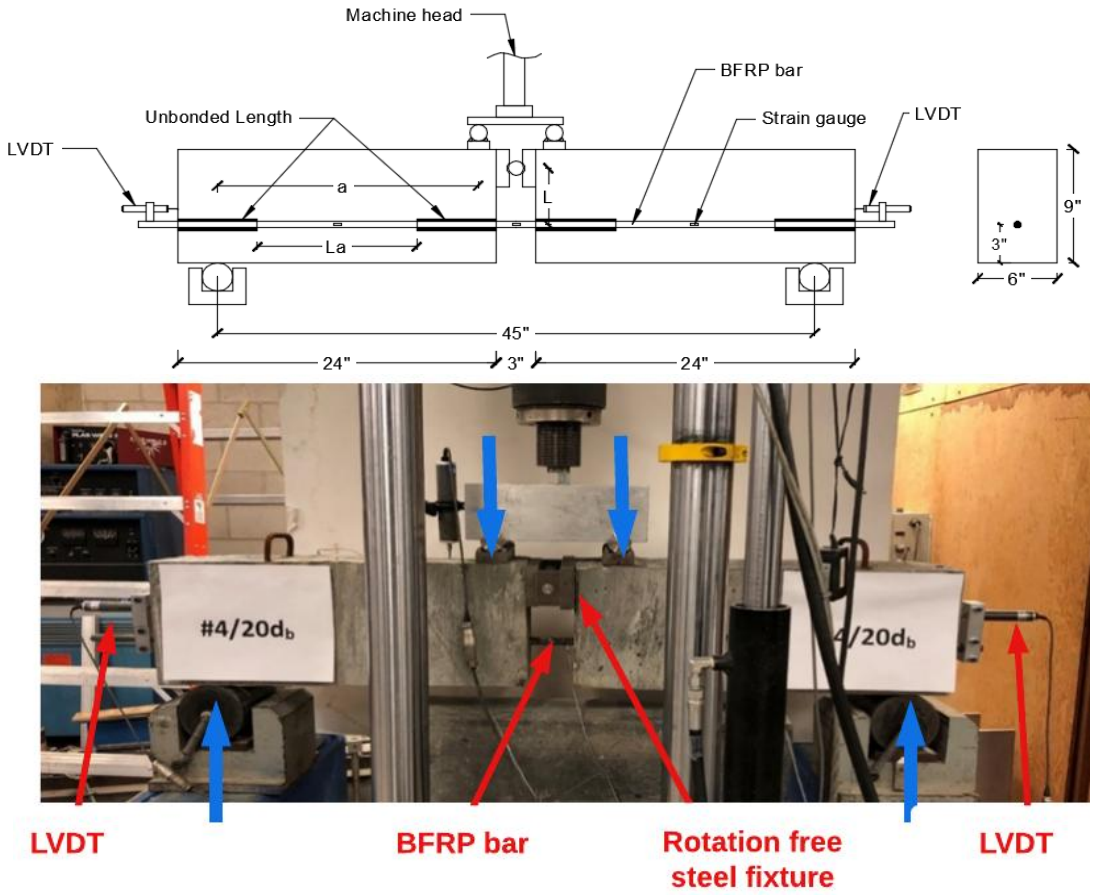

Bond strength

- Based on the bond strength data, the minimum development length should be **$39d_b$**, **$40d_b$**, and **$37d_b$** for bar sizes No. 4, 5, and 6, respectively.

$$l_e = \frac{A_f f_f}{u_f \pi d_b}$$

Where l_e development length
A_f bar area, in^2
u_f bond strength, psi
d_b bar diameter, in.

Bar size	Sample No.	Maximum tensile force, kips	Bonded area, in^2	Maximum bond stress, psi	Average bond stress, psi	Standard deviation, psi	Coefficient of variation, %
4	1	14.9	11.77	1266	1136	108	9.5
	2	12.2	11.77	1032			
	3	18.6	15.7	1181			
	4	16.7	15.7	1065			
5	1	21.2	18.4	1150	1109	42	3.7
	2	25.8	18.4	1054			
	3	27.0	24.5	1101			
	4	20.8	24.5	1131			
6	1	29.5	26.5	1111	1086	76	6.9
	2	28.1	26.5	1054			
	3	35.4	35.3	1000			
	4	41.6	35.3	1178			

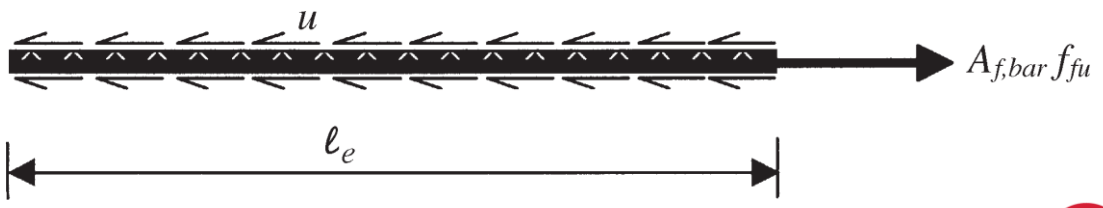

UIC ENGINEERING

Transverse shear strength

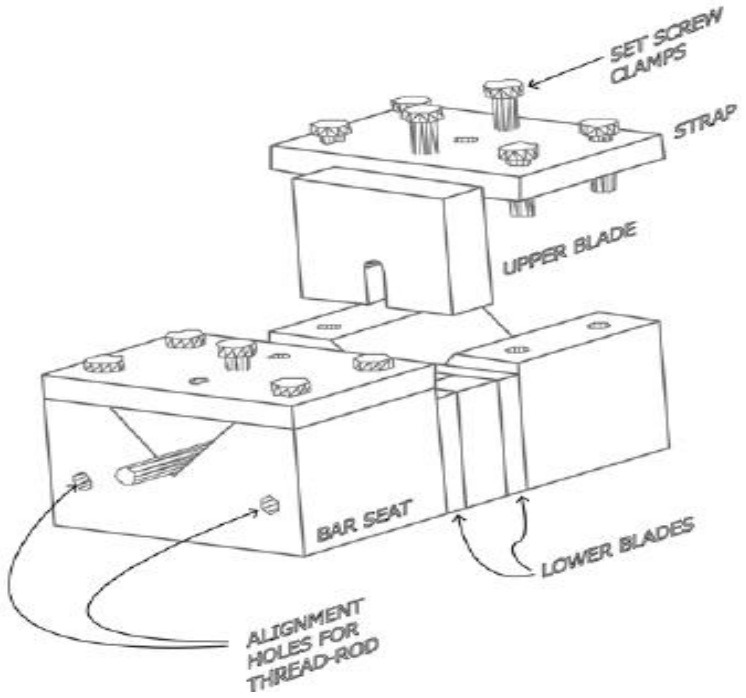

The transverse shear stress exerted on the BFRP bar can be calculated by the following equation:

$$\tau_u = \frac{P_s}{2A}$$

where τ_u is the transverse shear strength, psi, P_s applied load, lbs., A bar area, in^2.

Bar #	Sample #	Maximum applied force, kips	Shear area, in^2	Maximum shear stress, psi	Average shear stress, psi	Standard deviation, psi	Coefficient of variation, %
4	1	12.2	0.40	30,349	29,465	1528	5.1
	2	12.2	0.40	30,469			
	3	11.2	0.40	27,947			
	4	12.4	0.40	30,888			
	5	11.0	0.40	27,671			
5	1	20.0	0.62	32,289	31,447	1398	4.4
	2	21.0	0.62	33,823			
	3	19.2	0.62	30,982			
	4	19.4	0.62	31,172			
	5	18.8	0.62	30,377			
	6	18.6	0.62	30,038			
6	1	24.4	0.88	27,771	28,757	1406	4.8
	2	26.0	0.88	29,509			
	3	24.2	0.88	27,947			
	4	27.2	0.88	30,888			
	5	24.4	0.88	27,671			

Mechanical properties

Normalized property is the bar diameter mechanical property divided by the #4 result.

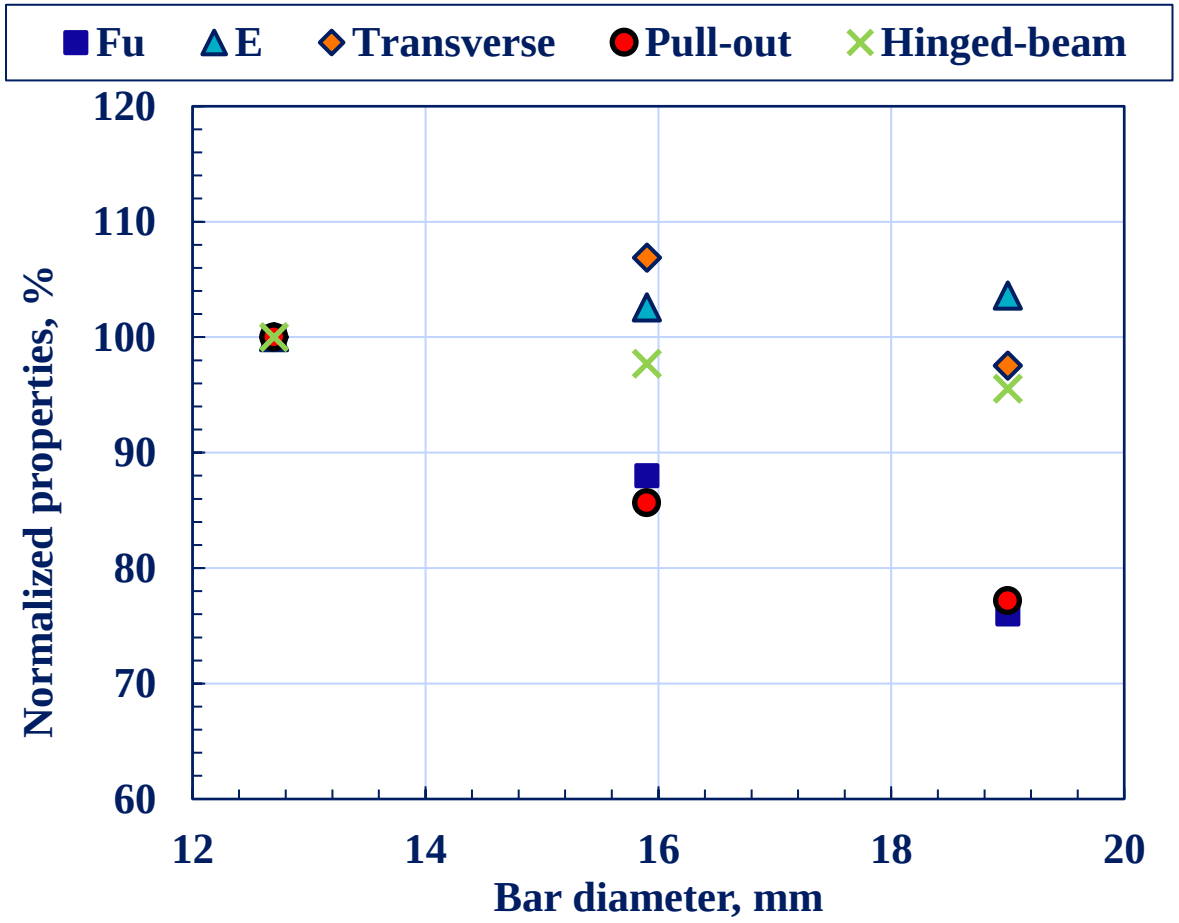

UIC ENGINEERING

Durability characteristics

- This study aims to investigate the degradation of strength due to exposure to the alkaline solution under constant temperature (60ºC).
- The solution comprises 118.5 g of $Ca(OH)_2$, 0.9 g of NaOH, and 4.2 g of KOH per 1 liter of deionized water, and the PH ranges between 12.6 and 13.0.

UIC ENGINEERING

Durability characteristics

- Tensile capacity retention is the tensile strength ratio after exposure to the tensile strength before exposure.

$$R_{et} = \frac{F_{tu1}}{F_{tu0}} \times 100$$

Bar size	Exposure time, months				
	0	1	2	3	6
#4	100	78.5	23.5	9.8	1.5
#5	100	83.5	59.6	44	30
#6	100	97.3	87.3	64.3	54

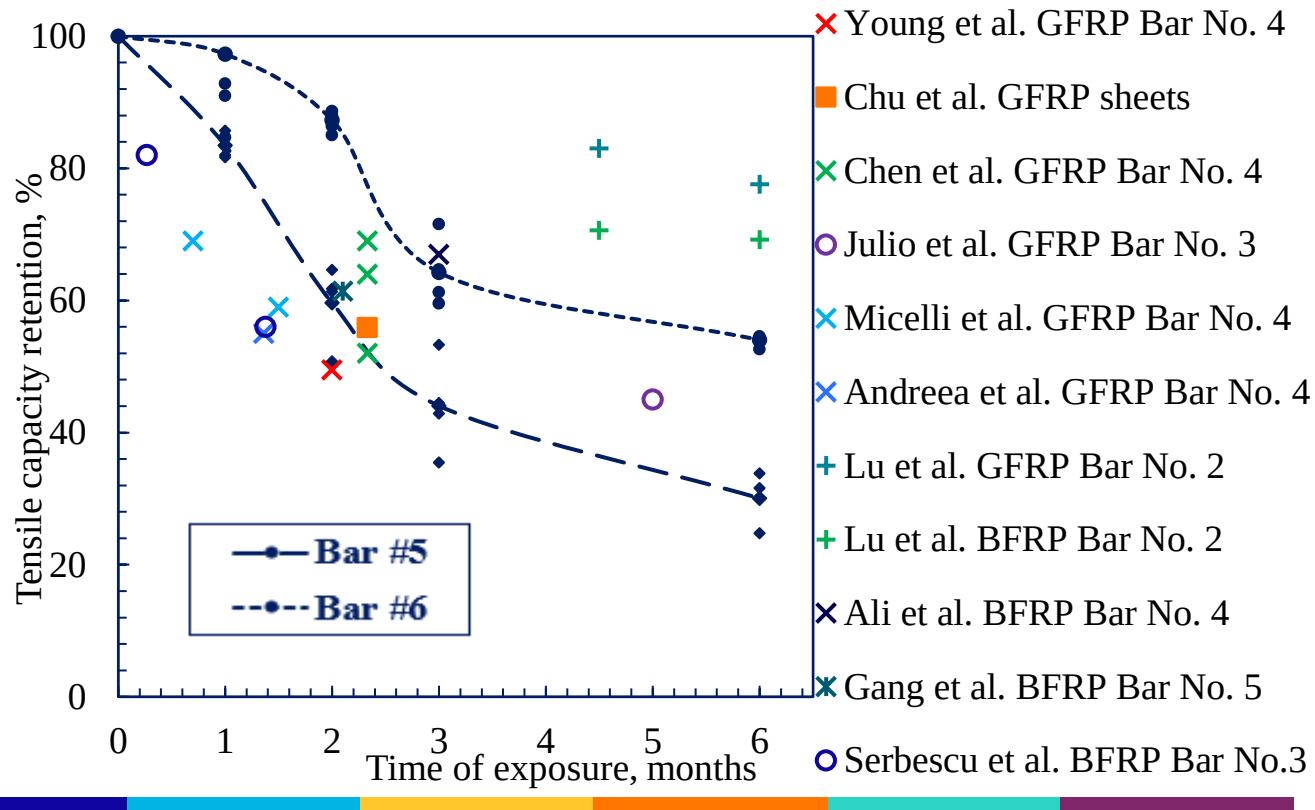

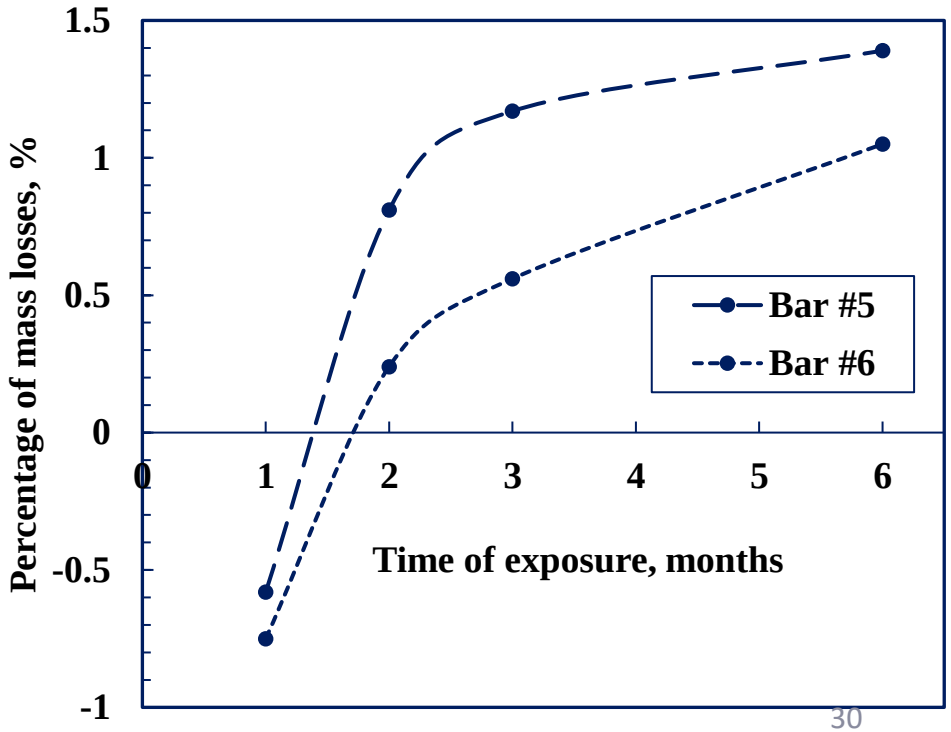

Durability characteristics (Predictive model)

- The aim of this predictive model is to compute the C_E (ACI440.1R) factor used in concrete design using FRP materials. This factor is the reduction factor of the bar ultimate strength due to environmental conditions.

- The two assumptions for this model are:

  1. The degradation onset is at PH7 and 20ºC.

  2. A conditioning period of 1,000 h is sufficient for the chemical reactions to stabilize and enable long-term predictions.

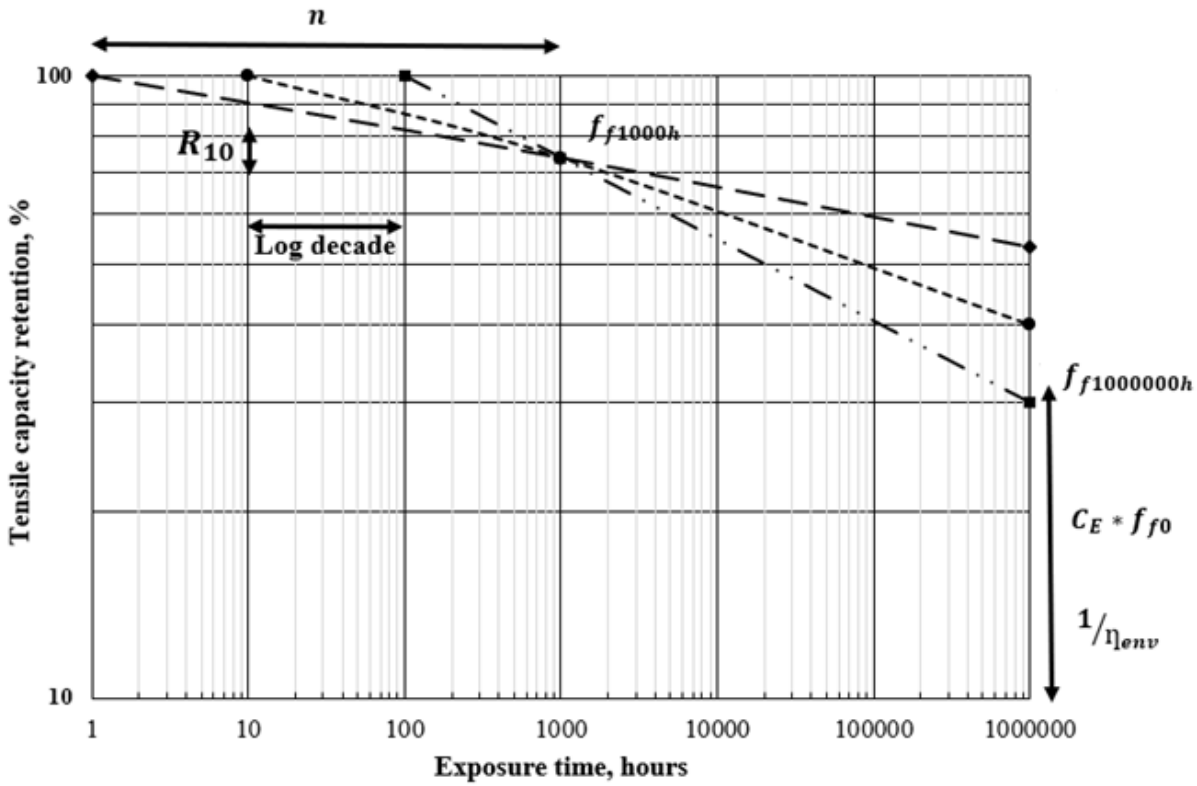

Durability characteristics (Predictive model)

- Degradation parameter n

$$n = n_{mo} + n_T + n_t + n_{pH} + n_d + n_{on} \geq 1 \quad \text{(no unit)}$$

- In this study, the tested rebars were conditioned in a saturated environment (n_{mo}= 1), pH = 13 (n_{pH} = 1), exposure time equal 1,000 h (n_t = 0), the diameter of the tested rebar for reference is equal to the conditioned rebar (n_d = 0), exposure temperature is 60ºC (n_T = 2.5), $f_{fk\ ref} = f_{fk0}$ (n_{on} = -1.5).

- This factor n (n=3) represents the position of the second point graphically connected to f_{f1000h} for the stress prediction.

Degradation parameter	Range	Value
Moisture RH (n_{mo})	Dry (50%)	-1
	Moist (80%)	0
	Saturated (100%)	1
PH (n_{pH})	7	0
	10	0.5
	13	1
Time (n_t)	≤1,000 h	0
	≥1,000 h	Log(h/1,000)
Diameter (n_d)	≥tested	0
	~75% tested	0.5
	~50% tested	1
Temperature (n_T)	0ºC	-0.5
	10ºC	0
	20ºC	0.5
	30ºC	1
	40ºC	1.5
	50ºC	2
	60ºC	2.5
Onset (n_{on})	$f_{fk\ ref} = f_{fk0}$	-1.5
	$f_{fk\ ref} \neq f_{fk0}$	$n_{on,opt}$

Durability characteristics (Predictive model)

$$m = \frac{\log(f_0) - \log(f_{f1000h})}{\log(1) - \log(1000)}$$

$$R_{10} = 100 - (10^m * 100)$$

$$n = n_{mo} + n_T + n_t + n_{pH} + n_d + n_{on}$$

$$\eta_{env} = {}^{1}/_{[(100 - R_{10})/100]^n}$$

$$f_{f,t\%} = ({}^{1}/_{\eta_{env}}) * 100$$

Time, years	Predicted tensile capacity retention for bar No. 5, %	Predicted tensile capacity retention for bar No. 6, %
25	**57**	**89**
50	**55**	**88**
114	**53**	**87**

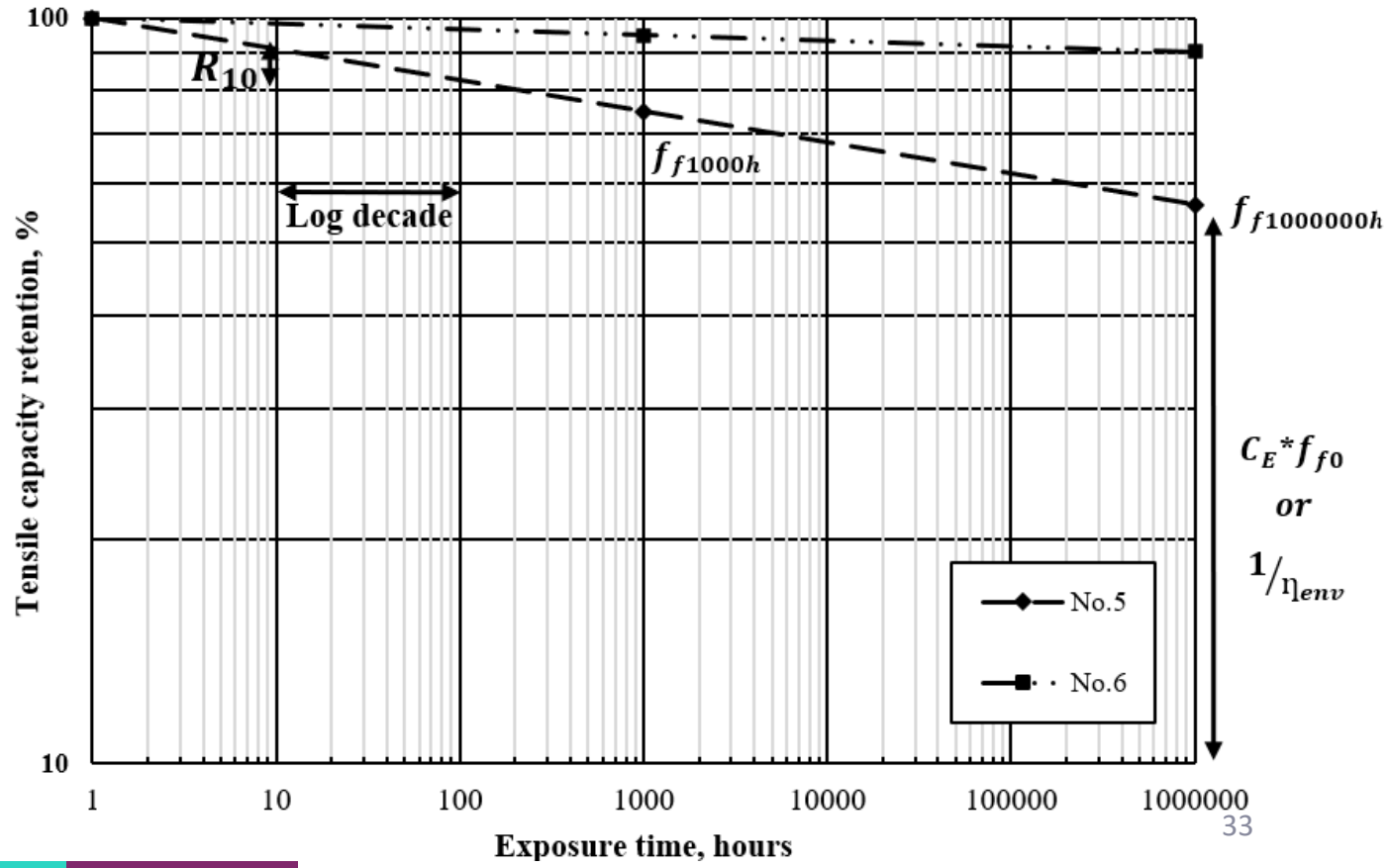

Durability characteristics (Freeze and thaw)

- This study investigates the freeze and thaw resistance of unidirectional pultrall BFRP bars from -4 ˚F to 73 ˚F for 100 cycles by freezing in air and thawing in water.

- The percentage of loss of bars #4, #5, and #6 are 3.1%, 7.4%, and 4.3%, with no significant mass loss.

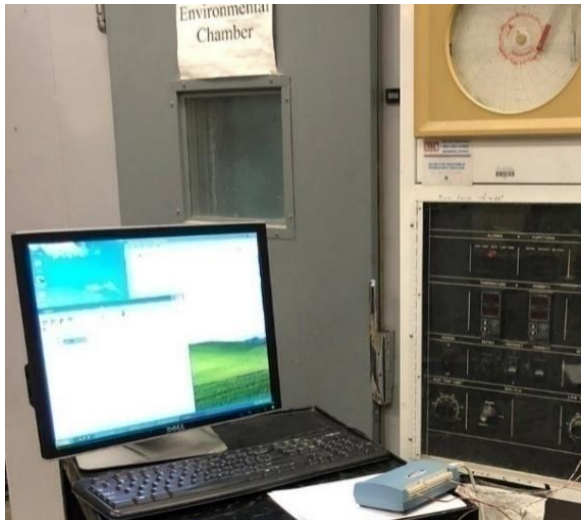

Bar #	Control specimens		Exposed specimens				Percentage of tensile stress loss, %
	Tensile modulus of elasticity, ksi	Tensile stress, ksi	Tensile modulus of elasticity, ksi	Tensile stress, ksi	Standard deviation, ksi	Coefficient of variation, %	
4	8494	226	8578	218.9	9.8	4.5	**3.1**
5	8674	202	8481	187.1	7.7	4.1	**7.4**
6	8798	171	8724	163.5	10.2	6.2	**4.3**

Outline

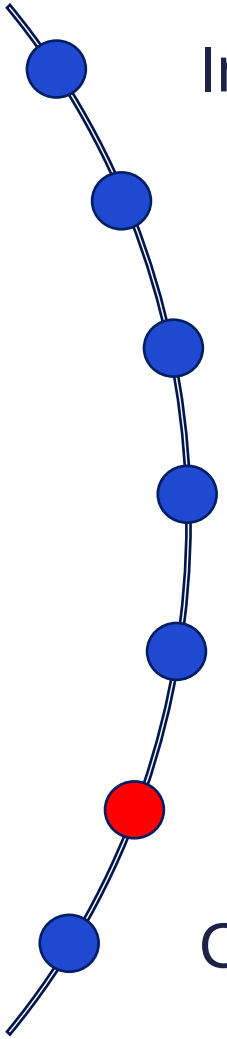

Introduction and Background of Basalt-FRP

Research Objectives

Research Approach

Literature Review

Basalt-FRP Material Properties

Structural behavior of Bridge Deck Slabs

Conclusions and Future work

UIC ENGINEERING

Structural Behavior of Bridge Deck Slabs Reinforced with Basalt-FRP Bars as Internal Reinforcement

UIC ENGINEERING

Structural behavior of bridge decks

- The second phase of this research is testing **six full-scale** bridge deck slabs under static loading of two different BFRP bar sizes, bar spacing, and continuity conditions.

- To the authors' best knowledge, only one research tested a bridge deck slab reinforced with a Basalt-FRP bar (Elgabbas et al., 2015).

(Elgabbas et al., 2015).

UIC ENGINEERING

Structural behavior of bridge decks

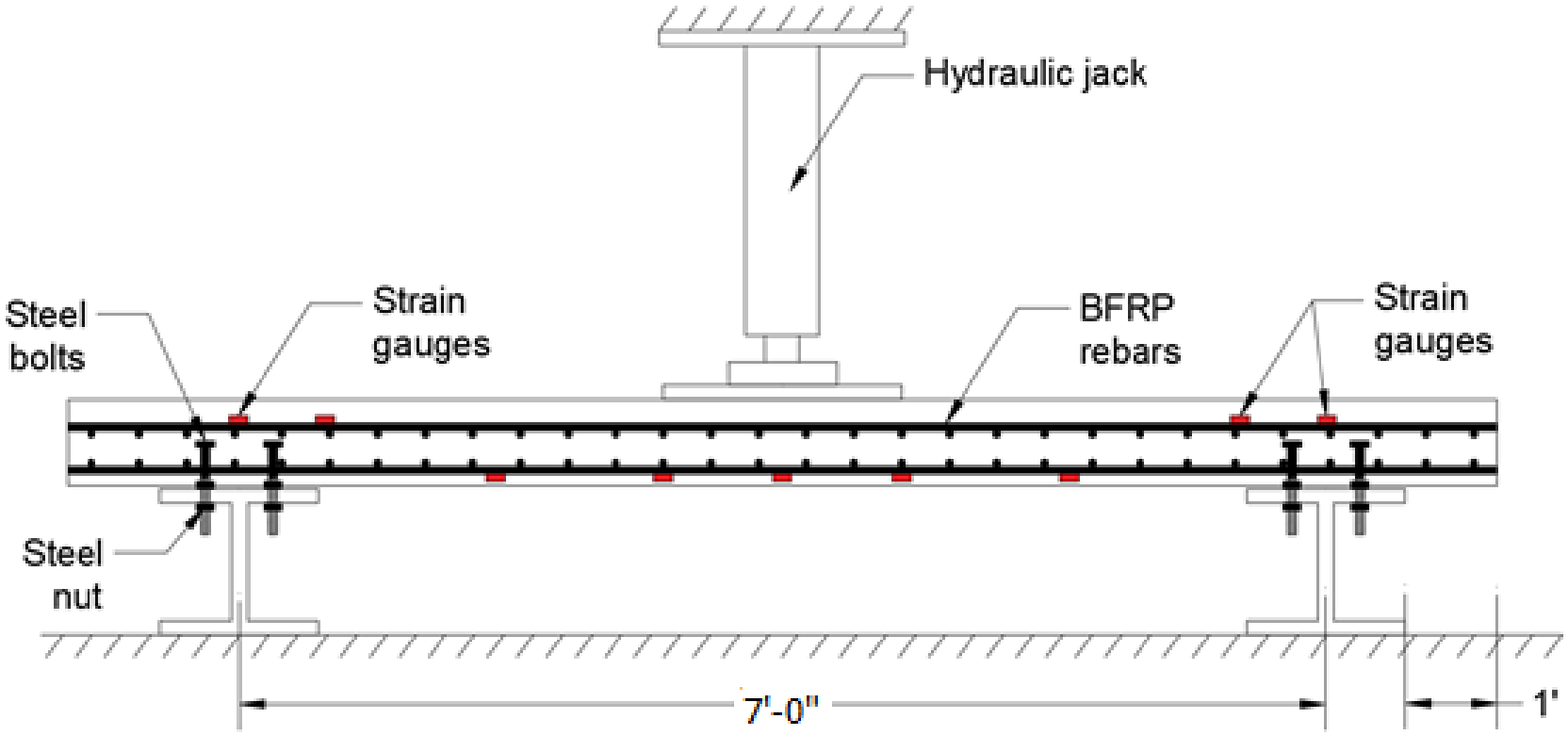

UIC ENGINEERING

Slabs design

Unlike steel, the BFRP reinforcement ratio must exceed the value of the balanced conditions due to the lower modulus of elasticity

$$\rho_{fb} = 0.85\beta_1 \frac{f'_c}{f_{fu}} \frac{E_f \varepsilon_{cu}}{E_f \varepsilon_{cu} + f_{fu}}$$

Bridge Deck Slabs	Length, ft	Width, ft	Continuity condition	Span length, ft	Transverse bottom reinforcement	Transverse top reinforcement	Longitudinal and transverse top reinforcement
SS1	10’	4’	Single-span	7’	No.5@4”	No.5@4”	No.5@4”
SS2	10’	4’	Single-span	7’	No.5@6”	No.5@6”	No.5@6”
SS3	10’	4’	Single-span	7’	No.5@8”	No.5@8”	No.5@8”
SS4	10’	4’	Single-span	7’	No.6@6”	No.5@6”	No.5@6”
TS5	18’	10’	Two-span	7.5’	No.5@4”	No.5@4”	No.5@6”
TS6	18’	10’	Two-span	7.5’	No.5@6”	No.5@6”	No.5@8”

UIC ENGINEERING

Slabs design

BFRP Design

$$\rho_{fb} = 0.85\beta_1 \frac{f'_c}{f_{fu}} \frac{E_f \varepsilon_{cu}}{E_f \varepsilon_{cu} + f_{fu}} \approx \mathbf{0.24\%}$$

- Flexural-shear failure
- Φ = 0.65 (Strength reduction factor)
- Over-reinforced section
- Reinforcement tensile strength ≈ 200ksi
- $n_f = \frac{E_f}{E_c} = 2.2$ (Modular ratio)

Steel Design

$$\rho_{fb} = 0.85\beta_1 \frac{f'_c}{f_y} \frac{\varepsilon_{cu}}{\varepsilon_{cu} + \varepsilon_s} \approx \mathbf{5.44\%}$$

- Failure in the tension zone
- Φ = 0.9 (Strength reduction factor)
- Under-reinforced section
- Reinforcement tensile strength = 60ksi
- $n_s = \frac{E_s}{E_c} = 7$ (Modular ratio)

UIC ENGINEERING

Slabs design

- The concrete compressive strength used in the slab ranges between 6.5 and 7.1 ksi with a water-cement ratio of 0.44, 6 inches slump, and 6% air-entrained.

Slab Prototype	f'_c ksi	Bar size	f_{fu} ksi	E_f , ksi	ε_{cu} in./in.	β_1	ρ_b %	ρ %	ρ/ρ_b
SS 1	7.12	#5	202	8673	0.003	0.69	0.237	1.159	**4.88**
SS 2	6.95	#5	202	8673	0.003	0.7	0.234	0.773	**3.3**
SS 3	6.5	#6	171	8798	0.003	0.72	0.313	1.107	**3.53**
SS 4	6.35	#5	202	8673	0.003	0.73	0.223	0.579	**2.59**
TS 5	6.95	#5	202	8673	0.003	0.7	0.234	1.159	**4.94**
TS 6	6.5	#5	202	8673	0.003	0.72	0.226	0.773	**3.42**

UIC ENGINEERING

Instrumentation plan

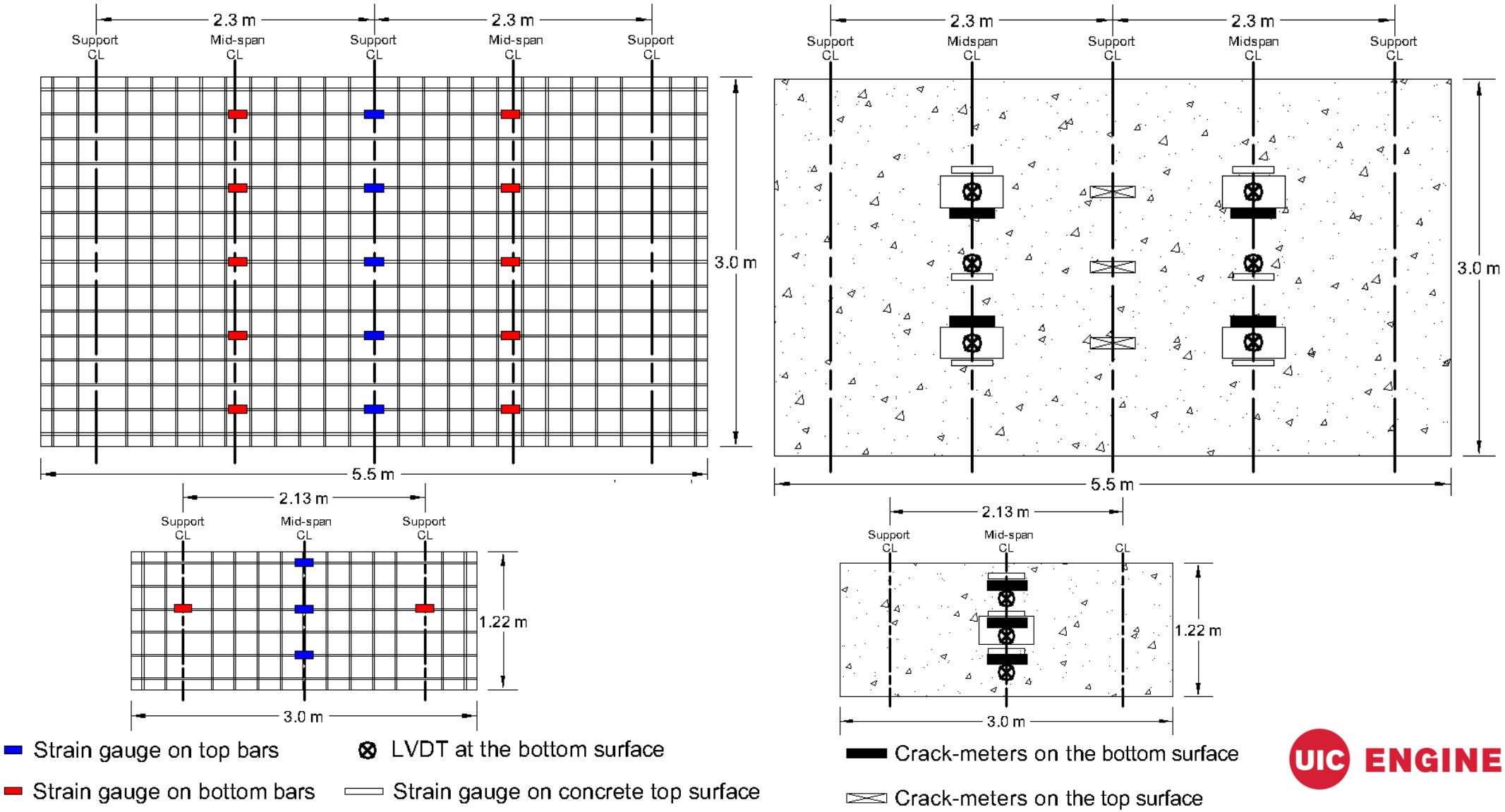

Structural behavior of bridge decks

- The single-span bridge deck was supported on two steel sections bolted to the steel bed.
- The slab thickness was selected to keep the ratio of supporting-beam spacing to slab thickness less than 12 and to represent the most commonly used size of the concrete bridge deck in North America.
- The width of the two-span bridge deck slab is 10 ft to account for the tandem loading with four points loading (2 on each midspan).
- Four-point loading will be applied to the slab with two points on each mid-span.

Tandem loading

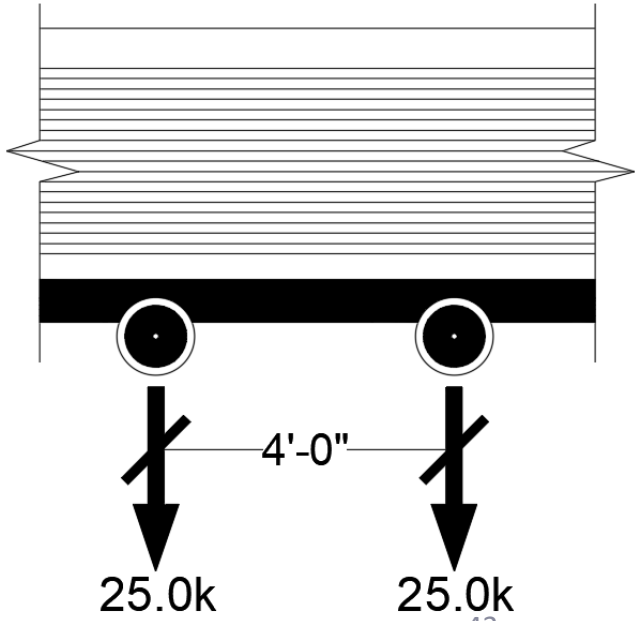

Testing setup

UIC ENGINEERING

Testing setup

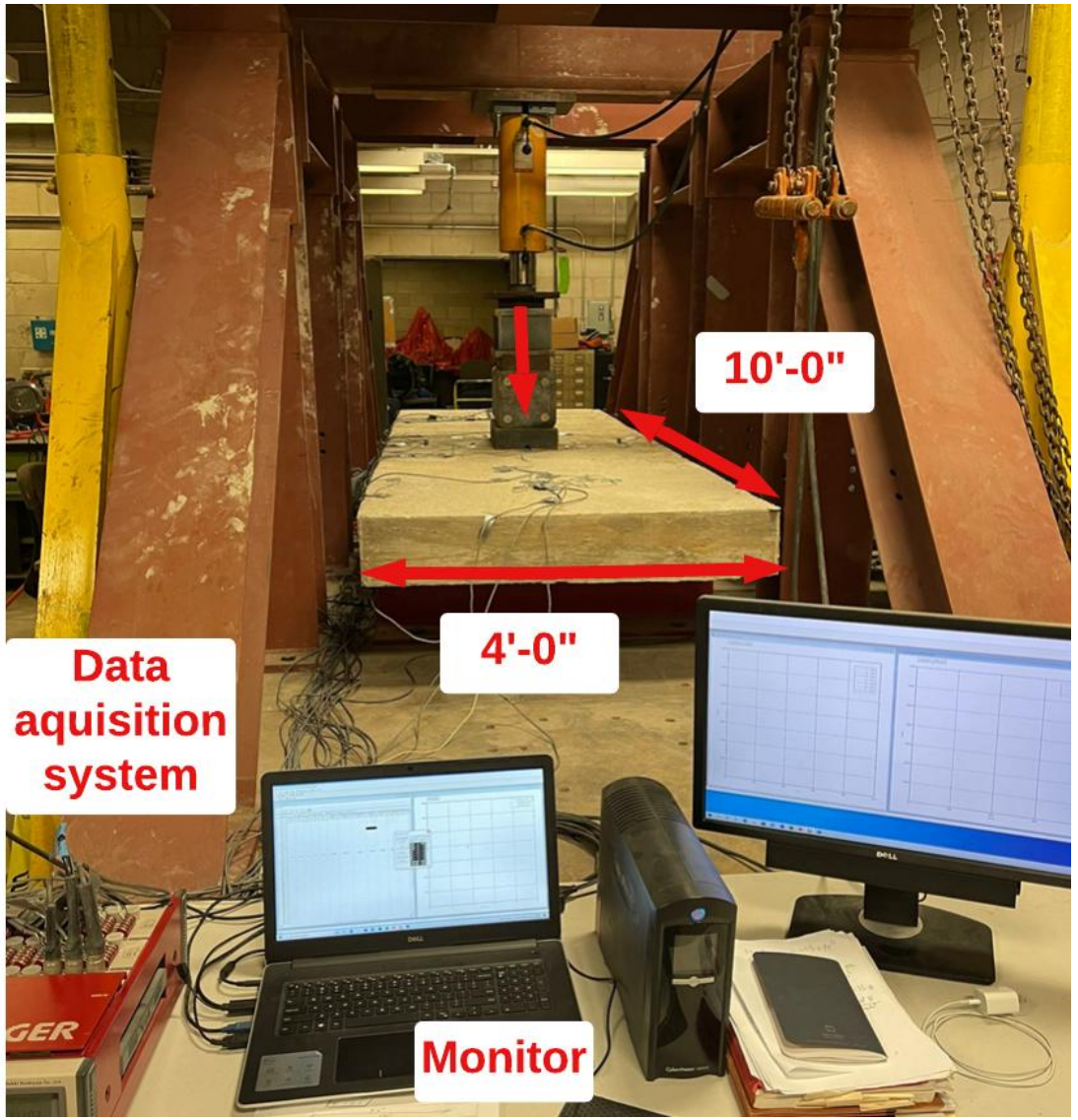

Testing setup

UIC ENGINEERING

Slab failure mode

UIC ENGINEERING

Slab failure mode

Slab failure mode

UIC ENGINEERING

Cracking load calculation

For the calculation of cracking load, the following calculation was derived:

$$\sigma_{cr} = \frac{M.c}{I} \quad , \quad I = \frac{b.h^3}{12} \quad , \quad c = \frac{h}{2} \quad , \quad \sigma_{cr} = 7.5 \times \sqrt{f'_c}$$

$$b = 12\ in. \qquad h = 8\ in. \qquad c = 4\ in.$$

$$P_{cr} = 3.68\ kips/\text{ft}$$

UIC ENGINEERING

Slab testing results

Slab Prototype	Cracking load, kips	Cracking load per foot, kips	Ultimate load, kips	Ultimate load per foot, kips	Failure mode
SS 1	13.5	**3.37**	130	**32.5**	Flexural-shear
SS 2	11.8	**2.97**	109	**27.4**	Flexural-shear
SS 3	14.2	**3.52**	129	**32.4**	Flexural-shear
SS 4	12.9	**3.20**	112	**28.0**	Flexural-shear
TS 5	33.0	**3.30**	241	**24.1**	Flexural-shear
TS 6	41.5	**4.18**	181	**18.1**	Flexural-shear

UIC ENGINEERING

Slab testing results

Slab Prototype	Deflection at cracking load, x10^{3}in	Maximum deflection at ultimate load, in	Strain in BFRP at cracking load, μƐ	Maximum strain in BFRP at ultimate load, μƐ	Strain in concrete at cracking load, μƐ	Maximum strain in concrete at ultimate load, μƐ	Maximum crack width at ultimate load, x10^{-3}in
SS 1	26.7	0.78	163	6549	87	1921	39.3
SS 2	29.5	0.92	269	7835	109	2339	67.3
SS 3	37.4	0.82	377	6187	168	2224	27.9
SS 4	21.5	1.05	133	10597	112	2951	127.6
TS 5	21.1	0.77	237	6720	92	1572	40.2
TS 6	22.8	0.66	330	6604	143	1961	43.3

UIC ENGINEERING

Slab testing results

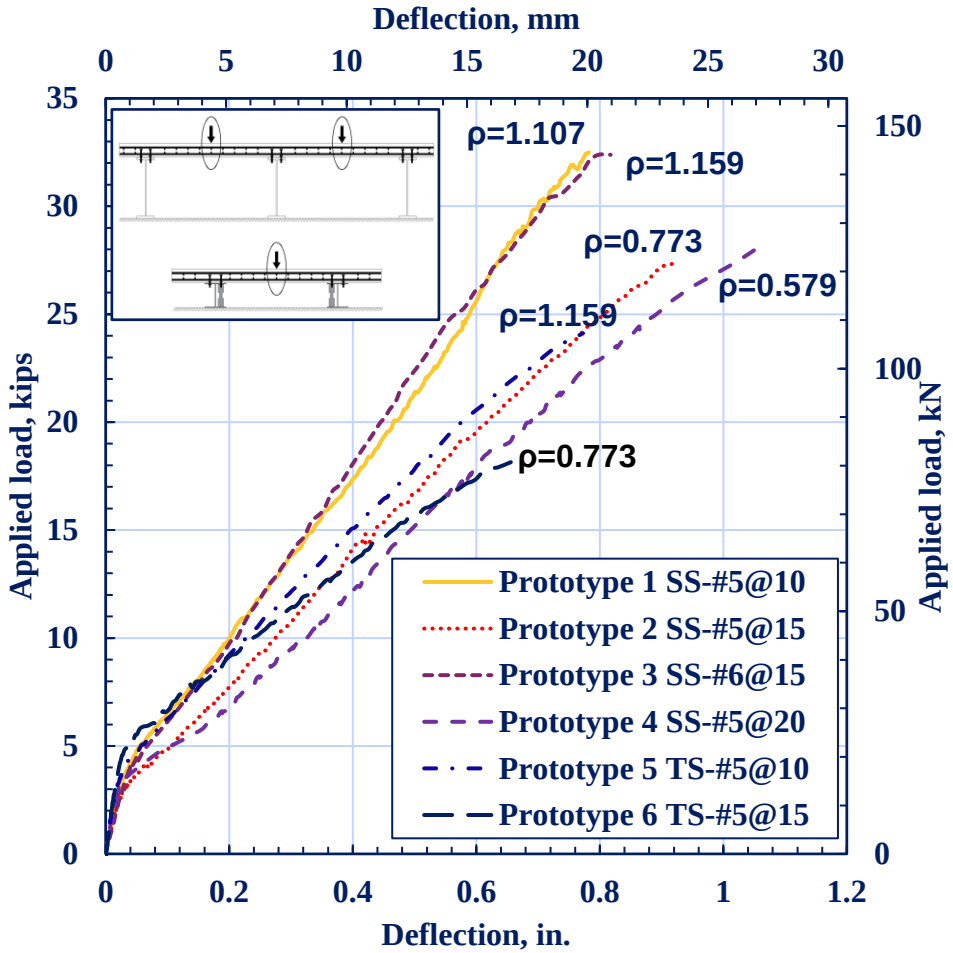

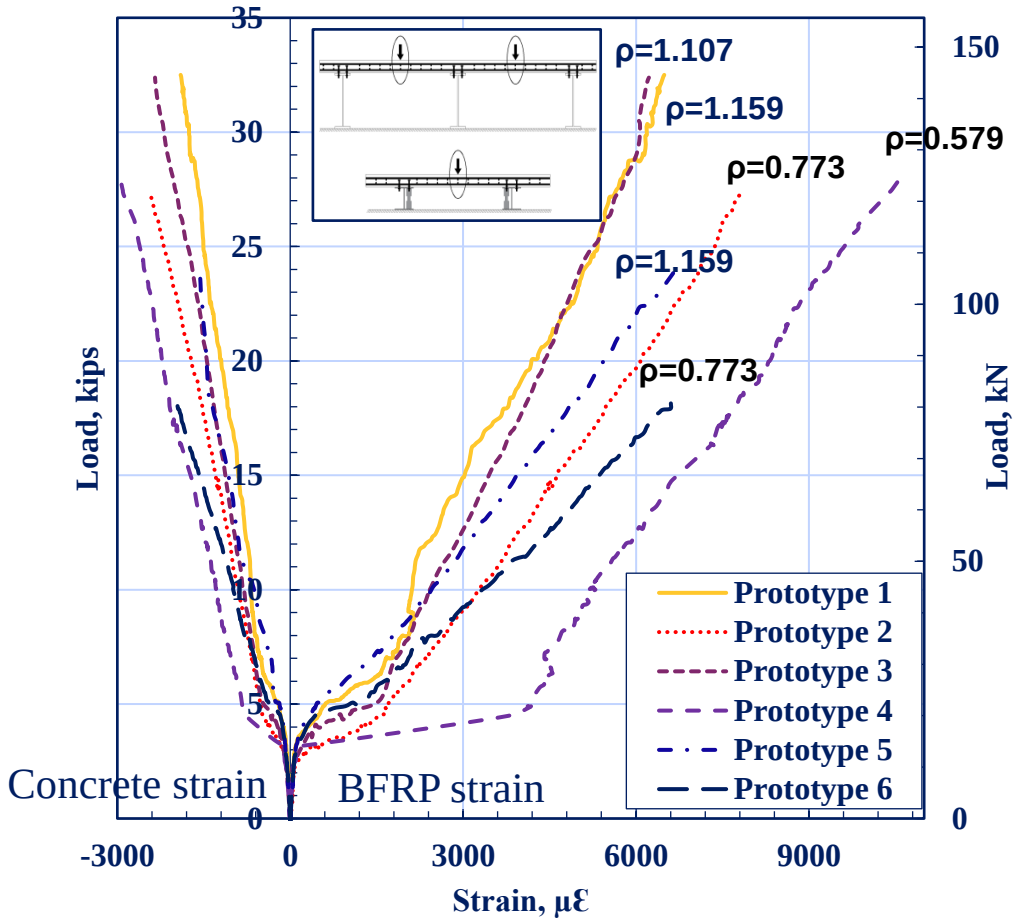

UIC ENGINEERING

Slab testing results

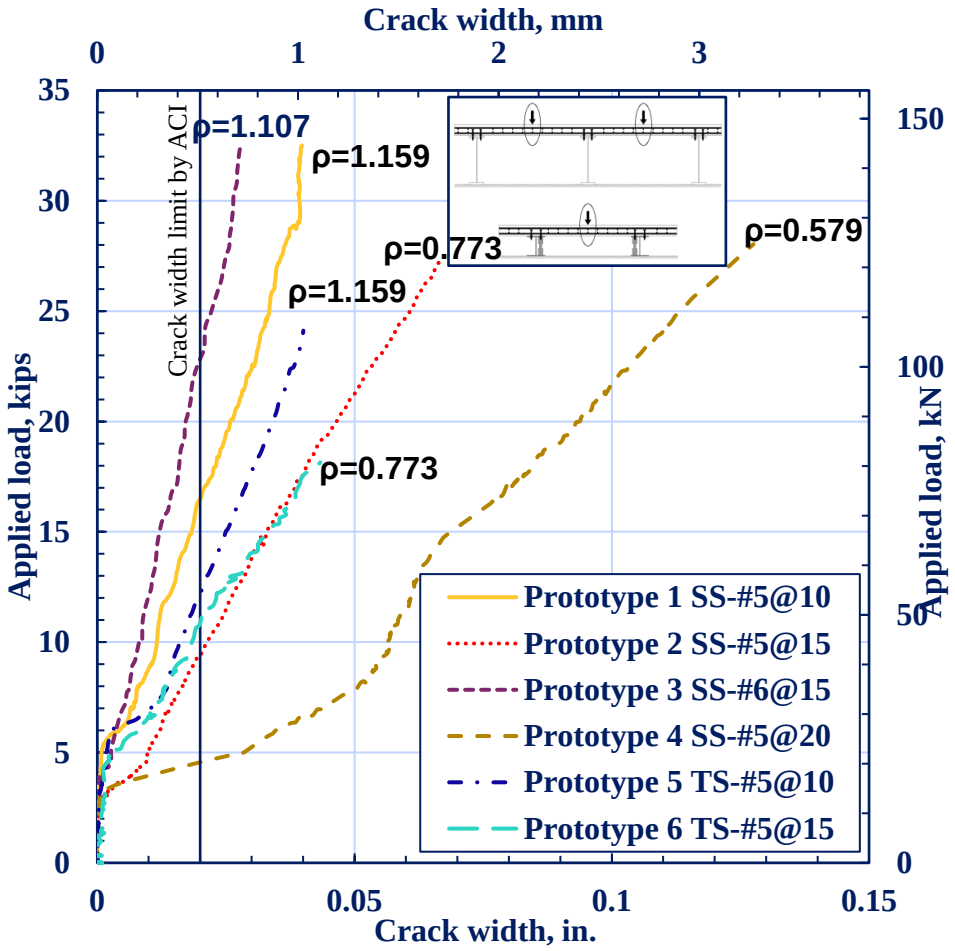

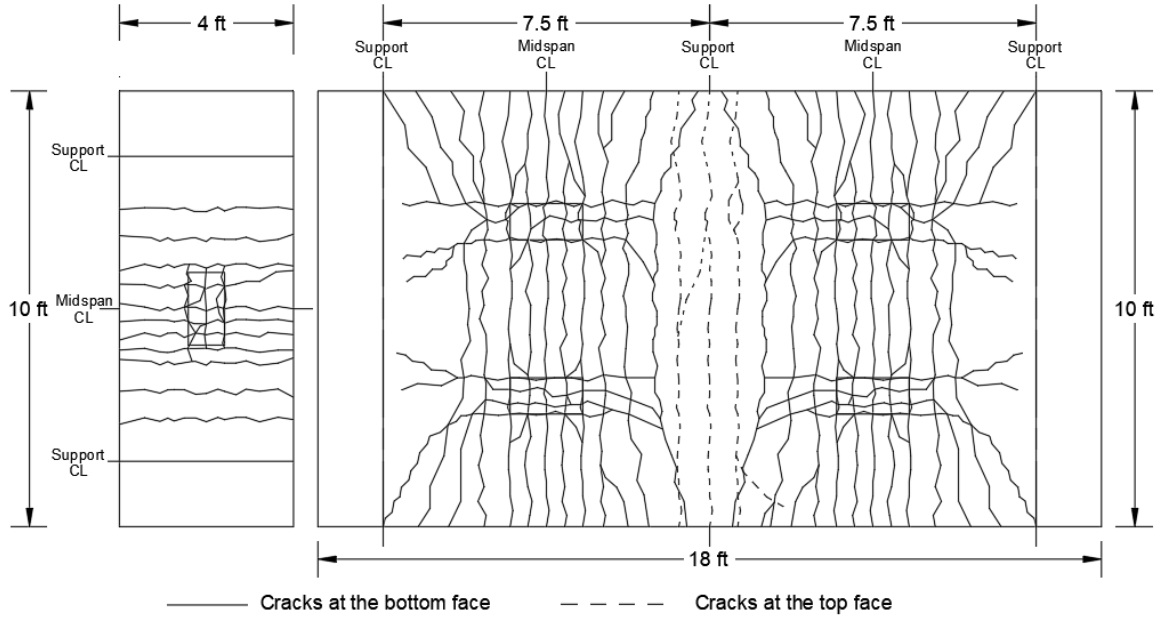

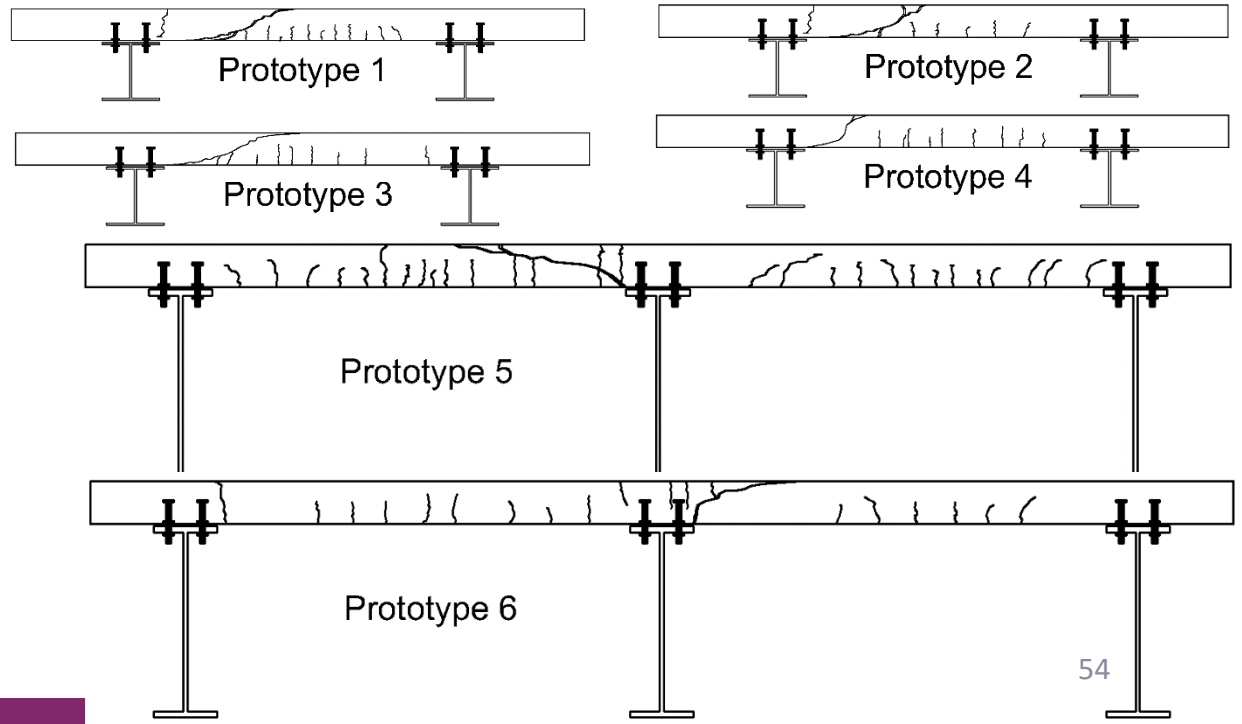

Structural behavior of bridge decks (proposed design equation)

- Several predictive models have been generated to account for the punching shear capacity of bridge deck slabs reinforced with FRP bars (El-Gamal et al., 2005, Peled et al., 1999, Ospina et al., 2003, El-Ghandour et al., 1999).

- Since bridge deck slabs have been designed as a flexural element, it is essential to study the flexural shear capacity for a better understanding of the behavior and to ease the design of the bridge deck using FRP materials as a main reinforcement.

- ACI440.1R existing equation:

$$V_{c,ACI440.1R} = \frac{2}{5}\sqrt{f'_c}\, b_0 k d \quad ; \quad k = \sqrt{2\rho_f n_f + (\rho_f n_f)^2} - \rho_f n_f$$

UIC ENGINEERING

Structural behavior of bridge decks (proposed design equation)

Parameters in the proposed equation

- Span length
- Concrete compressive strength
- Modulus of elasticity of FRP bars
- Reinforcement ratio

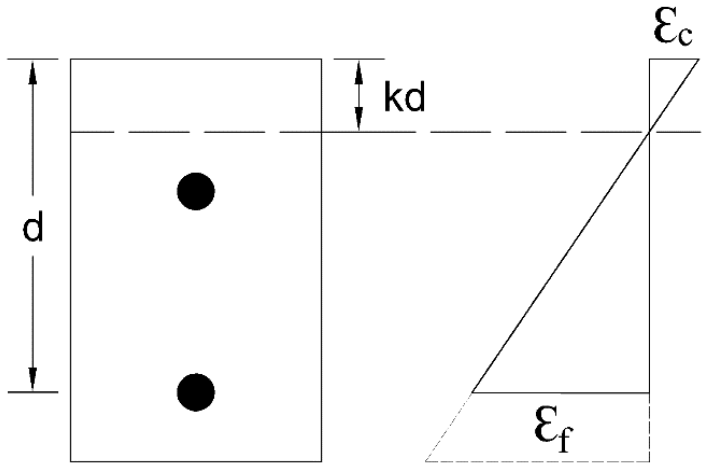

UIC ENGINEERING

Structural behavior of bridge decks (proposed design equation)

Parameters in the proposed equation

- Span length
- Concrete compressive strength
- Modulus of elasticity of FRP bars
- Reinforcement ratio

$$V_c = \frac{2}{5}\sqrt{f'_c}\, b_0 kd\, \alpha\, (1.2)^N$$

Where

$$\alpha = 10\left(\frac{1}{\rho}\right)^{0.415}\left(\frac{1}{S}\right)^{2.216}\left(\frac{1}{E_f}\right)^{0.261}\left(\frac{1}{f'_c}\right)^{0.122}$$

UIC ENGINEERING

Structural behavior of bridge decks

The proposed equation was validated using four research projects from the literature that used FRP bars as the main reinforcement in bridge decks.

- El-Sayed et al.
- Zheng et al.
- Pantelides et al.
- Yost et al.
- Present study

Reference		V_{test} kN (kips)	b_0, m (ft)	d, cm (in)	f'c, MPa (ksi)	ρ, %	Spanm (ft)	E_f GPa (ksi)	N	ACI440.1R-15 V_{theort}	ACI440.1R-15 V_{test}/V_{theort}	Proposed equation V_{theort}	Proposed equation V_{test}/V_{theort}
El-Sayed et al.	S-C1	140 (31.5)	1 (3.3)	16.6 (6.5)	40 (5.8)	0.39	2.5 (8.2)	114 (16534)	0	66.6 (15)	2.10	163.7 (36.8)	0.86
	S-C2B	167 (37.5)	1 (3.3)	16.6 (6.5)	40 (5.8)	0.78	2.5 (8.2)	114 (16534)	0	90.9 (20.4)	1.84	167.5 (37.7)	1.00
	S-C3B	190 (42.7)	1 (3.3)	16.6 (6.5)	40 (5.8)	0.12	2.5 (8.2)	114 (16534)	0	38.1 (8.56)	4.99	153.8 (34.6)	1.24
	S-G1	113 (25.4)	1 (3.3)	16.6 (6.5)	40 (5.8)	0.86	2.5 (8.2)	40 (5801)	0	59.2 (13.3)	1.91	137.6 (31.0)	0.82
	S-G2	142 (31.9)	1 (3.3)	16.6 (6.5)	40 (5.8)	1.7	2.5 (8.2)	40 (5801)	0	80.7 (18.1)	1.76	141.4 (31.8)	1.00
	S-G2B	163 (36.6)	1 (3.3)	16.6 (6.5)	40 (5.8)	1.71	2.5 (8.2)	40 (5801)	0	80.9 (18.2)	2.01	141.4 (31.8)	1.15
	S-G3	163 (36.6)	1 (3.3)	16.6 (6.5)	40 (5.8)	2.44	2.5 (8.2)	40 (5801)	0	94.7 (21.3)	1.72	142.7 (32.1)	1.14
	S-G3B	168 (37.8)	1 (3.3)	16.6 (6.5)	40 (5.8)	2.63	2.5 (8.2)	40 (5801)	0	97.8 (22.0)	1.72	143.0 (32.1)	1.18
Zheng et al.	CG10	107.5 (24.2)	0.5 (1.6)	16 (6.3)	73 (10.6)	0.3	2.14 (7)	44.6 (6469)	0	21.4 (4.81)	5.02	98.4 (22.1)	1.09
	CG11	105.5 (23.7)	0.5 (1.6)	16 (6.3)	71.7 (10.4)	0.7	2.14 (7)	44.6 (6469)	0	31.9 (7.17)	3.31	103.2 (23.2)	1.02
	CG12	111.5 (25.1)	0.5 (1.6)	16 (6.3)	74.4 (10.8)	1.4	2.14 (7)	44.6 (6469)	0	44.4 (10.0)	2.51	107.2 (24.1)	1.04
	CG14	92.5 (20.8)	0.5 (1.6)	16 (6.3)	29.52 (4.28)	0.7	2.14 (7)	44.6 (6469)	0	25.1 (5.64)	3.68	90.6 (20.4)	1.02
	CG15	100 (22.8)	0.5 (1.6)	16 (6.3)	56 (8.12)	0.7	2.14 (7)	44.6 (6469)	0	29.9 (6.72)	3.35	99.5 (22.4)	1.00
	CG16	99.5 (22.4)	0.5 (1.6)	16 (6.3)	67.7 (9.82)	0.7	2.14 (7)	44.6 (6469)	0	31.4 (7.06)	3.17	102.3 (23.2)	0.97
	CG19	99.5 (22.4)	0.5 (1.6)	16 (6.3)	75.37 (10.9)	0.7	2.14 (7)	44.6 (6469)	0	32.3 (7.26)	3.08	103.9 (23.4)	0.96
Pantelides et al.	SP-1-NW	119 (26.7)	0.61 (2)	20.2 (7.95)	60 (8.7)	0.65	2.44 (8)	43.3 (6280)	0	44.6 (10.0)	2.67	114.8 (25.8)	1.04
	SP-2-NW	132 (29.7)	0.61 (2)	20.2 (7.95)	71 (10.3)	0.65	2.44 (8)	43.3 (6280)	0	46.6 (10.0)	2.83	117.7 (26.5)	1.12
	SP-3-NW	130 (29.2)	0.61 (2)	20.2 (7.95)	89 (12.9)	0.65	2.44 (8)	43.3 (6280)	0	49.5 (11.1)	2.63	121.5 (27.3)	1.07
	SP-4-LW	108 (24.3)	0.61 (2)	20.2 (7.95)	63 (9.1)	0.65	2.44 (8)	43.3 (6280)	0	45.2 (10.2)	2.39	115.6 (26.0)	0.93
	SP-5-LW	99 (22.2)	0.61 (2)	20.2 (7.95)	60 (8.7)	0.65	2.44 (8)	43.3 (6280)	0	44.6 (10.0)	2.22	114.8 (25.8)	0.86
	SP-6-LW	99 (22.2)	0.61 (2)	20.2 (7.95)	75 (10.9)	0.65	2.44 (8)	443.3 (6280)	0	47.3 (10.6)	2.09	118.6 (26.7)	0.83
Yost et al.	H1	218 (49)	1.22 (4)	17.7 (6.97)	33 (4.79)	2.26	2.44 (8)	41.3 (5990)	0	114.4 (25.7)	1.90	190.8 (42.9)	1.14
	H2	160.5 (36.0)	1.22 (4)	17.7 (6.97)	33 (4.79)	2.26	2.44 (8)	41.3 (5990)	0	114.4 (25.7)	1.40	190.8 (42.9)	0.84
	H3	173.5 (39)	1.22 (4)	17.7 (6.97)	33 (4.79)	2.26	2.44 (8)	41.3 (5990)	0	114.4 (25.7)	1.52	190.8 (42.9)	0.91
	C1	232 (52.2)	1.22 (4)	0.18 (7.09)	33 (4.79)	2.48	2.44 (8)	85 (12328)	0	163.9 (36.8)	1.42	217.7 (48.9)	1.07
	C2	213 (47.9)	1.22 (4)	0.18 (7.09)	33 (4.79)	2.48	2.44 (8)	85 (12328)	0	163.9 (36.8)	1.30	217.7 (48.9)	0.98
	C3	201 (45.2)	1.22 (4)	0.18 (7.09)	33 (4.79)	2.48	2.44 (8)	85 (12328)	0	163.9 (36.8)	1.23	217.7 (48.9)	0.92
Present study	P1	289 (65.0)	1.22 (4)	17 (6.69)	49.1 (7.12)	1.16	2.13 (7)	59.8 (8674)	0	107.5 (24.2)	2.69	275.5 (62.0)	1.05
	P2	242 (54.4)	1.22 (4)	17 (6.69)	47.9 (6.95)	0.77	2.13 (7)	59.8 (8674)	0	88.8 (20.0)	2.72	270.2 (60.7)	0.90
	P3	289 (65.0)	1.22 (4)	16.8 (6.61)	44.8 (6.5)	1.11	2.13 (7)	60.7 (8798)	0	102.4 (23.0)	2.82	269.4 (60.6)	1.07
	P4	249 (55.5)	1.22 (4)	17 (6.69)	43.8 (6.35)	0.58	2.13 (7)	59.8 (8674)	0	75.9 (17.1)	3.28	263.2 (59.2)	0.95
	P5	740 (166)	3.0 (10)	17 (6.69)	47.9 (6.95)	1.16	2.3 (7.5)	59.8 (8674)	1	266.9 (60.0)	2.77	706.5 (159)	1.04
	P6	545 (122)	3.0 (10)	17 (6.69)	44.8 (6.5)	0.73	2.3 (7.5)	59.8 (8674)	1	212.5 (47.8)	2.56	687.1 (154)	0.79
Average											2.50		**1.00**
SD											0.906		0.109
COV, %											36		**10.9**

Structural behavior of bridge decks (proposed design equation)

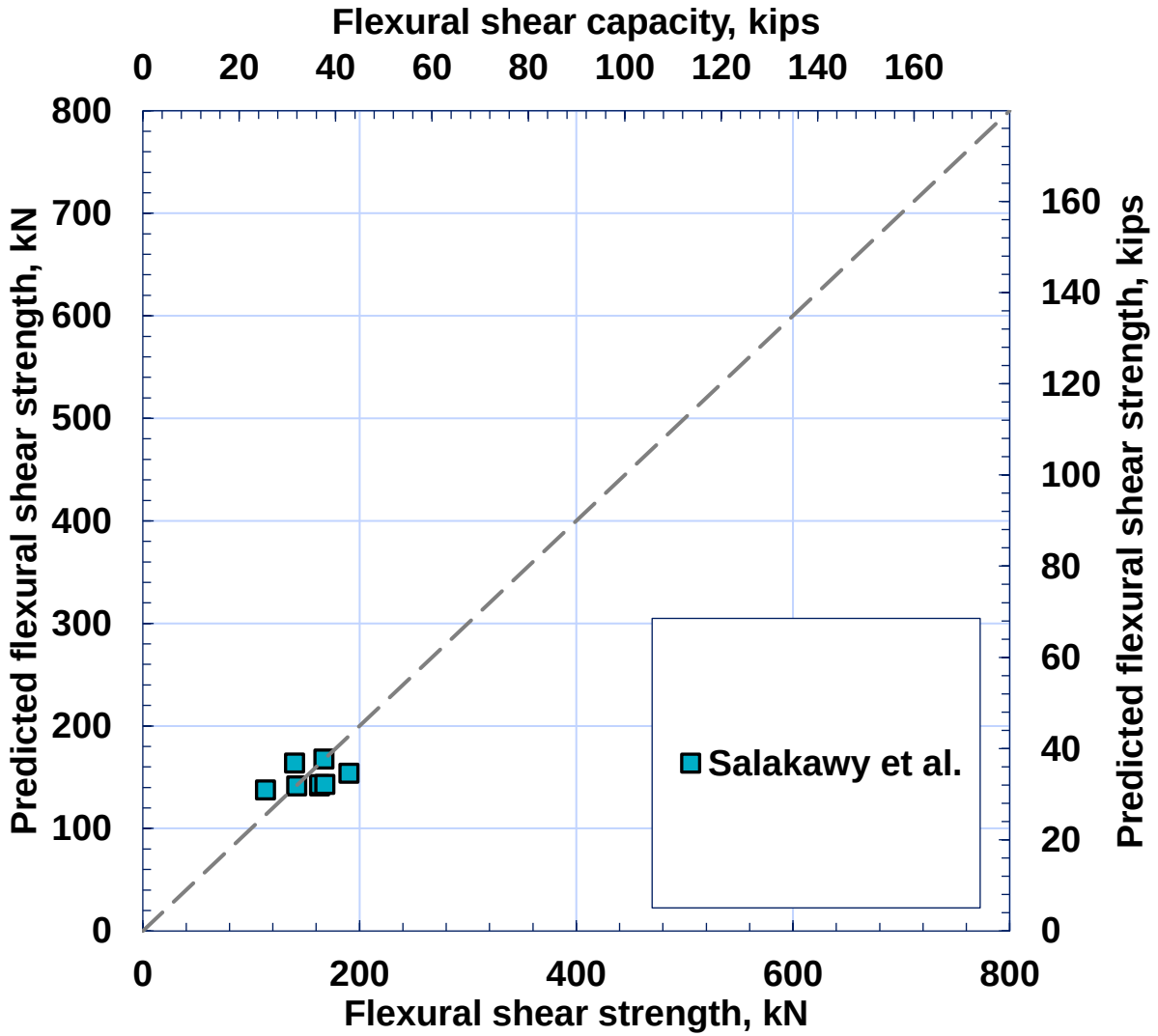

- The more the point is close to the y=x, the more accurate the equation is.
- The average ratio of the proposed flexural capacity to the experimental results is 1.00 compared to 2.5 with ACI, with a coefficient of variation of 10.8% compared to 36% in the ACI equation.
- The only red point shown in the figure represents Prototype 6 in the present study, which was expected to have higher capacity.

UIC ENGINEERING

Structural behavior of bridge decks (proposed design equation)

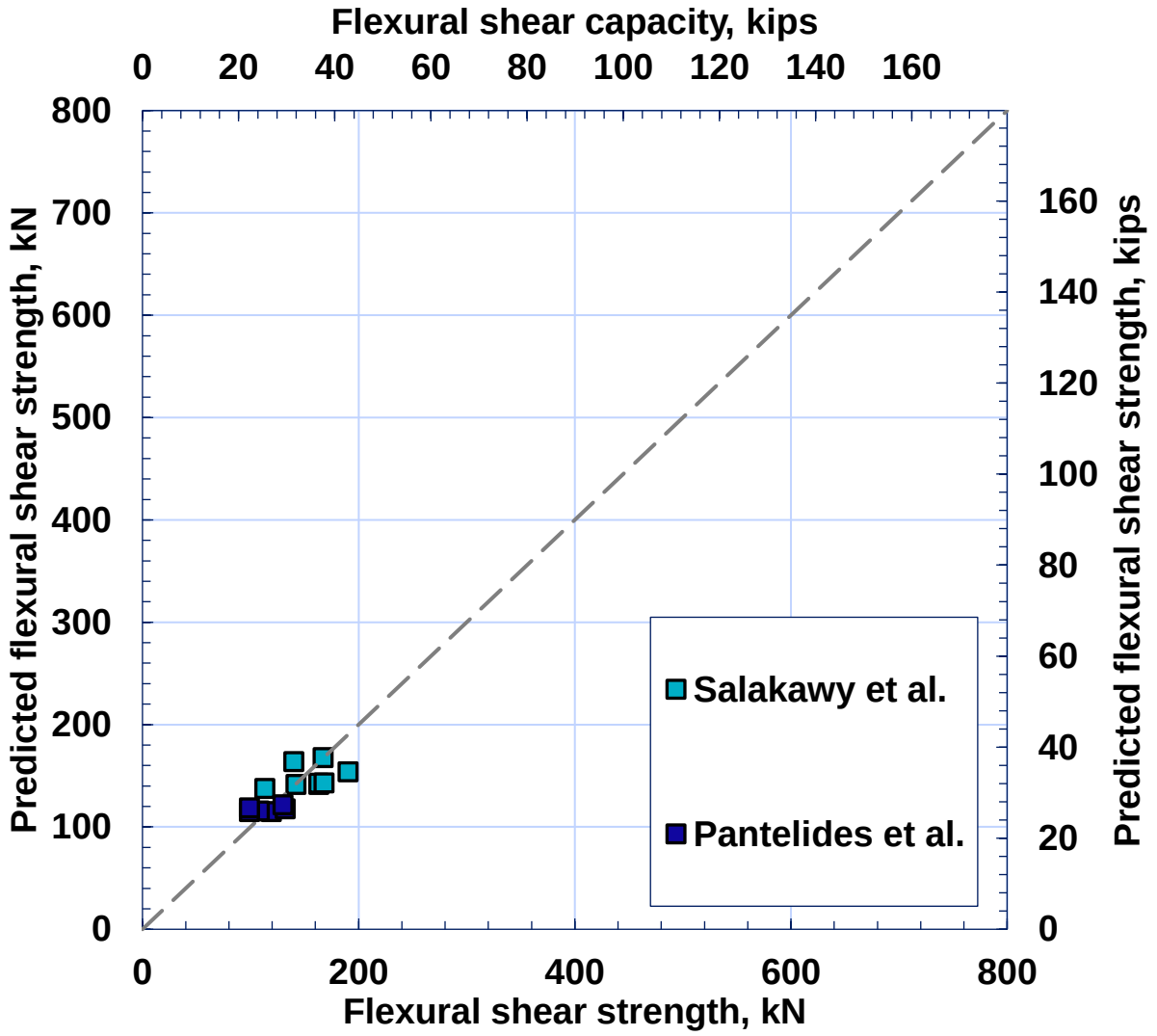

- The more the point is close to the y=x, the more accurate the equation is.
- The average ratio of the proposed flexural capacity to the experimental results is 1.00 compared to 2.5 with ACI, with a coefficient of variation of 10.8% compared to 36% in the ACI equation.
- The only red point shown in the figure represents Prototype 6 in the present study, which was expected to have higher capacity.

UIC ENGINEERING

Structural behavior of bridge decks (proposed design equation)

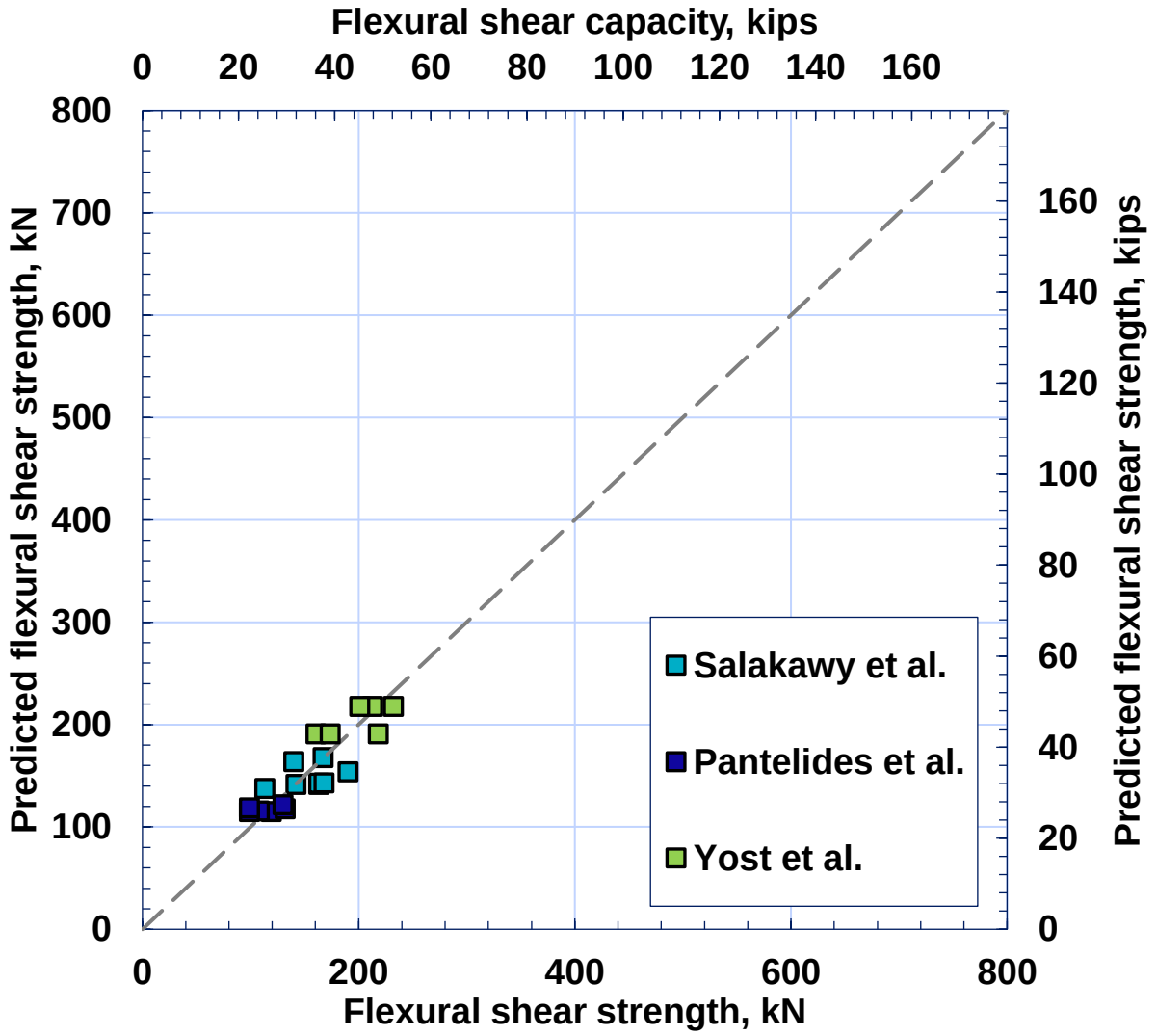

- The more the point is close to the y=x, the more accurate the equation is.
- The average ratio of the proposed flexural capacity to the experimental results is 1.00 compared to 2.5 with ACI, with a coefficient of variation of 10.8% compared to 36% in the ACI equation.
- The only red point shown in the figure represents Prototype 6 in the present study, which was expected to have higher capacity.

UIC ENGINEERING

Structural behavior of bridge decks (proposed design equation)

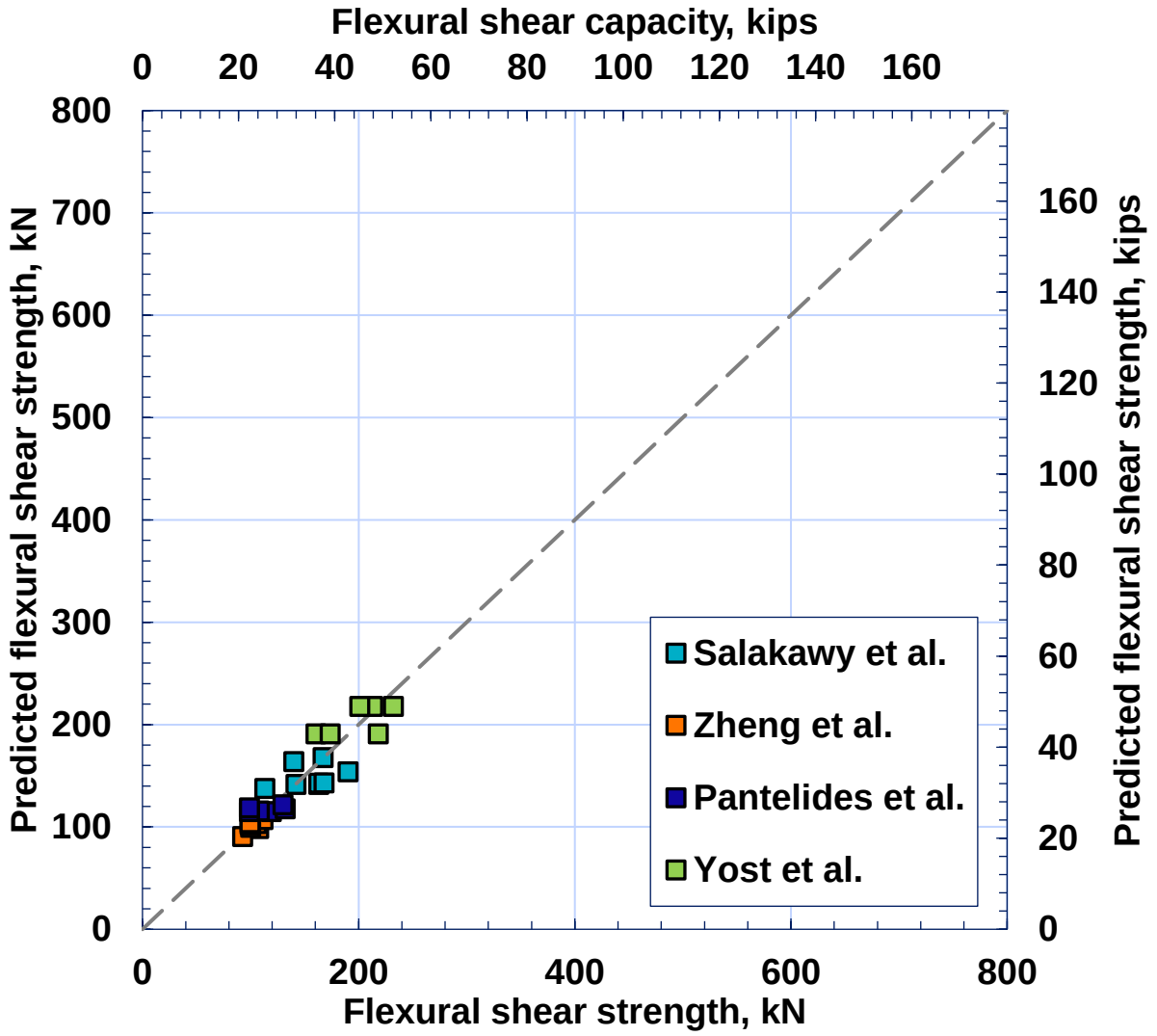

- The more the point is close to the y=x, the more accurate the equation is.
- The average ratio of the proposed flexural capacity to the experimental results is 1.00 compared to 2.5 with ACI, with a coefficient of variation of 10.8% compared to 36% in the ACI equation.
- The only red point shown in the figure represents Prototype 6 in the present study, which was expected to have higher capacity.

UIC ENGINEERING

Structural behavior of bridge decks (proposed design equation)

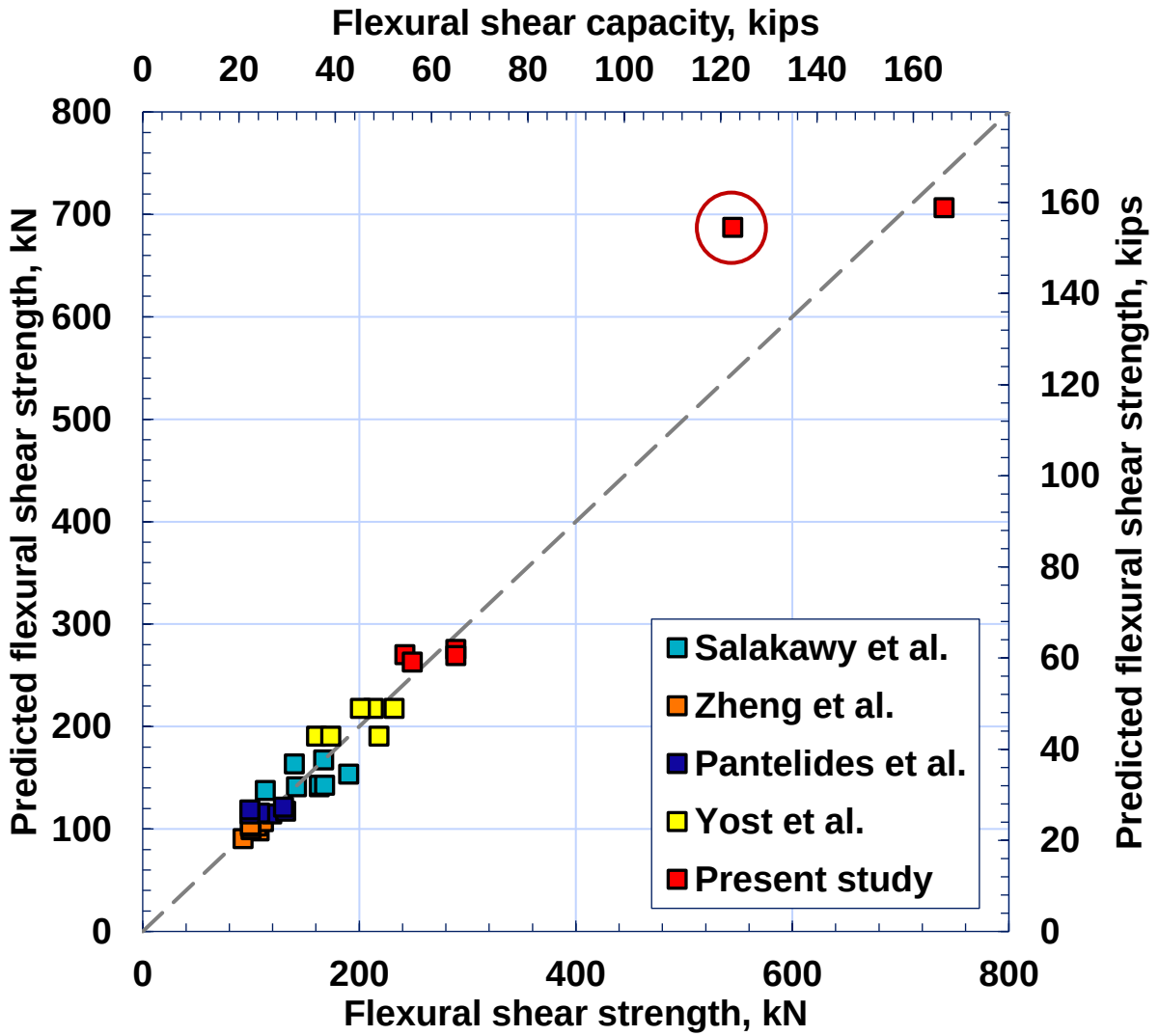

- The more the point is close to the y=x, the more accurate the equation is.
- The average ratio of the proposed flexural capacity to the experimental results is 1.00 compared to 2.5 with ACI, with a coefficient of variation of 10.8% compared to 36% in the ACI equation.
- The only circled point shown in the figure represents Prototype 6 in the present study, which was expected to have higher capacity.

UIC ENGINEERING

Structural behavior of bridge decks (proposed design equation)

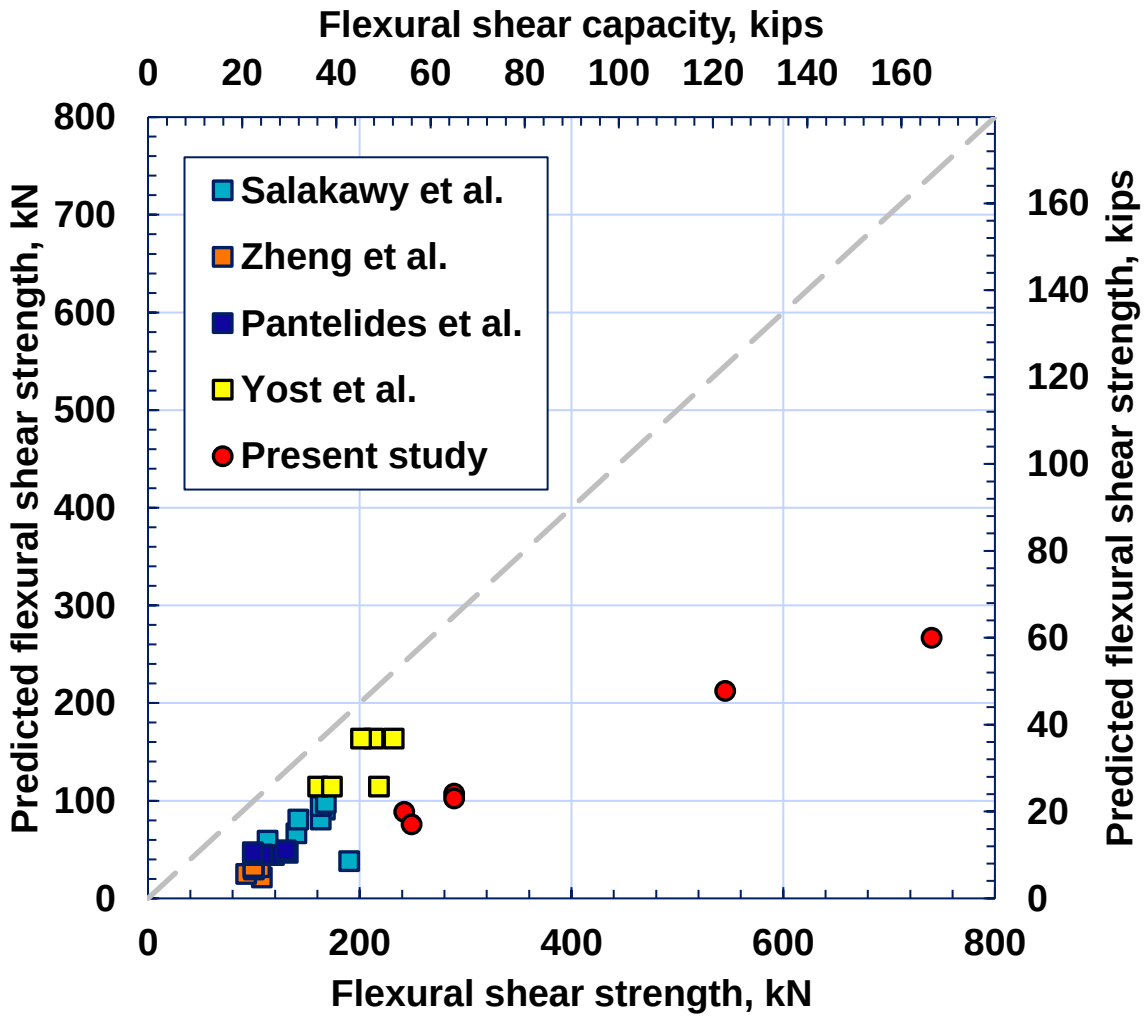

- The more the point is close to the y=x, the more accurate the equation is.
- The average ratio of the proposed flexural capacity to the experimental results is 1.00 compared to 2.5 with ACI, with a coefficient of variation of 10.8% compared to 36% in the ACI equation.
- The only red point shown in the figure represents Prototype 6 in the present study, which was expected to have higher capacity.

UIC ENGINEERING

Outline

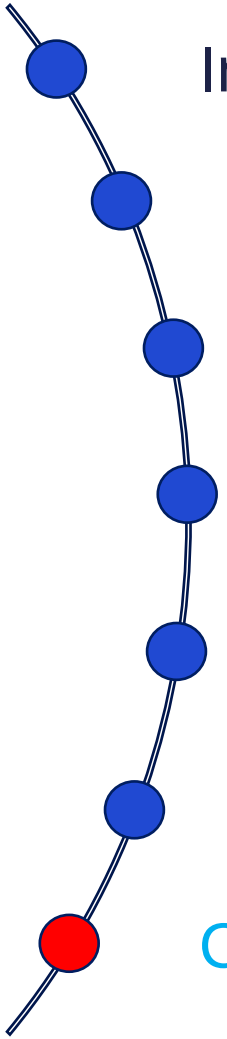

Introduction and Background of Basalt-FRP

Research Objectives

Research Approach

Literature Review

Basalt-FRP Material Properties

Structural behavior of Bridge Deck Slabs

Conclusions and Future work

UIC ENGINEERING

Conclusions

As an outcome of this research, the following conclusions have been derived:

- The impact of bar size on the mechanical properties of Basalt-FRP bars was found to vary. While ultimate **tensile strength** increased with larger bar sizes, **bond strength and tensile modulus of elasticity decreased**. However, shear strength and fiber content remained consistent regardless of bar size.
- The impact of exposure to alkaline on durability was found to vary depending on the size of the bar, according to the results. The BFRP bar **#6** was found to retain **87%** of its ultimate tensile strength, while **#5** retained **53%**, as predicted by the model. Despite this, the BFRP bars were found to have a high resistance to freeze and thaw cycles, and their tensile strength did not decrease significantly.
- When studying concrete bridge decks reinforced with Basalt-FRP bars, it was discovered that flexural-shear failure was the most common type of failure. An **empirical equation** was created to calculate the ultimate carrying capacity, which showed a high level of agreement with existing literature data, with a coefficient of variation of **10.8%**.

UIC ENGINEERING